Calculating the Global Flux of Carbon Dioxide into Groundwater

by

Toby Jonathan Kessler

B.A., Geology (1998)

University of Pennsylvania

Submitted to the Department of Earth, Atmospheric, and Planetary Sciences
as Part of the Requirements for the Degree of Master of Science in Geosystems

at the
Massachusetts Institute of Technology
May 1999

© 1999 Massachusetts Institute of Technology
All rights reserved

Signature of Author.....
Department of Earth, Atmospheric, and Planetary Sciences
May 10, 1999

Certified by.....
Charles F. Harvey
Associate Professor of Civil and Environmental Engineering
Thesis Supervisor

Accepted by.....
Ronald G. Prinn, Department Chairman

MASSACHUSETTS INSTITUTE OF TECHNOLOGY
WITHDRAWN
JUN 01 1999
MIT LIBRARIES
LIBRARIES

Table of Contents

	Page
Acknowledgements	3
List of figures and tables	4
Abstract	7
Introduction	8
Background	
Global climate change	10
Dissolution of CO_2 into water	11
Soils	14
Groundwater recharge	17
Holdridge life-zones	19
Methods	
Methods summary	21
Chemistry of carbonate system	23
Data gathering methods	
PCO_2	28
pH estimation	29
Climate and hydrologic parameters	30
Error in parameters	31
Regressions	32
Depth correction	34
Results	37
Discussion	40
Conclusion	43
Figures	44
Tables (except for table 5: p. 25, and table 9: p. 31)	73
Bibliography	85

Acknowledgements

Dr. Charles Harvey advised me and provided much of framework for this research and collected most of the papers with PCO_2 data. Dr. Michael Follows helped with the formulation of the chemistry, and with the background about the carbon cycle. The Carbon Dioxide Information and Analysis Center in Oak Ridge, TN, sent several materials related to the carbon cycle, and Rik Leemans sent a database that he created for the Holdridge Life-zone classification system. This thesis was done for the Geosystems master's degree program, and I received numerous pieces of advise from many others involved with the program.

Figures and Tables

Figure 1. Diagram showing the path of CO_2 in the ground with the focus of this study at the water table.

Figure 2. The global carbon cycle, showing the reservoirs in gigatons of carbon (GtC) and fluxes in GtC/y, as annual averages from 1980 to 1989. (Houghton 1995)

Figure 3. The ratio of fugacity (fCO_2) to PCO_2 between 270 and 320 Kelvin (DOE 1994)

Figure 4. Soil horizons from a road cut in central Africa (Brady 1996)

Figure 5. The formation of clays and oxides of iron and aluminum by the weathering of bedrock.

Figure 6. Groundwater recharge (R_g) for the Western Hemisphere. The larger numbers on the map are references to particular rivers, and the smaller numbers are R_g values in mm/y. The names on the map are in Russian, although the text of the book is translated. (L'vovich 1979)

Figure 7. World map of the Holdridge life-zones (Emanuel 1985)

Figure 8. Classification scheme for the Holdridge life-zones. The vertical axis is temperature and the two diagonal axes are precipitation and potential evapotranspiration ratio. (Holdridge 1972)

Figure 9. Biotemperature plotted as contours, as a function of temperature and latitude

Figure 10. Locations of PCO_2 measurements used in this study

Figure 11. K_h as a function of temperature (Plummer 1982)

Figure 12. K_1 as a function of temperature (Plummer 1982)

Figure 13. K_2 as a function of temperature (Plummer 1982)

Figure 14. DIC (mol/l) shown in contours, as a function of pH and temperature (K). One can see that for pH below about 5.5, the DIC is not sensitive to changes in pH. For higher pH, DIC is more sensitive to pH changes. Temperature does not have as great an effect.

Figure 15. Geographic distribution of pH in U.S. soils. The bold numbers are means for the selected areas, while the small numbers are county average concentrations. (Holmgren 1993)

Figure 16. Land resource areas corresponding to **Table 7** (Holmgren 1993)

Figure 17. Generalized soil map of the world from Report No. 66, 1991, FAO, printed in Bridges (Bridges 1997)

Figure 18. Generalized soil map of the world with U.S. soil classification system (Service 1994)

Figure 19. Graphs showing PCO_2 as a function of depth and time for three different crops grown in Mexico (Buyanovsky 1983)

Figure 20. Contours of PCO_2 as a function of depth and time at Brighton, Utah (Solomon 1987)

Figure 21. Graph of PCO_2 as a function of depth for a soil in Saskatchewan, Canada (Hendry 1993)

Figure 22. Derivation for PCO_2 versus depth profile, starting from the assumption of a uniform source of CO_2 throughout the soil profile

Figure 23. PCO_2 versus depth, as derived in **Figure 22**, for a single PCO_2 measurement of .01 atm, at a depth of 2 m, and atmospheric $PCO_2 = 10^{-3.5}$. The depth of the water table is 30 m.

Figure 24. Composite plot for PCO_2 as a function of depth, for data used in this study, with a linear regression line drawn to fit the data

Figure 25. Carbon Flux per Area, calculated for Holdridge life-zones

Figure 26. Regression for $\log(PCO_2)$ as a function of precipitation and biotemperature. PCO_2 from the regression is plotted as diagonal contour lines, and the measurements used in this study are plotted as stars

Figure 27. Linear regression between $\log(PCO_2)$ and precipitation

Figure 28. Linear regression between $\log(PCO_2)$ and temperature

Figure 29. Carbon flux calculated for the Holdridge temperature-regions (excluding the polar region)

Table 1. Geometric means of selected soil elements and associated soil parameters in U.S. surface soils by taxonomic soil order. (Holmgren 1993)

Table 2. PCO_2 measurements and their locations as plotted in **Figure 10**

Table 3. Complete set of parameters used for the calculations in this study

Table 4. Test to show that $K_1K_2/[H^+]^2$ and $K_w/[H^+]$ are negligible for realistic limits of T, pH, and PCO_2

Table 5. (Within text, page 25) Three possible ways of calculating DIC

Table 6. Comparisons between measured and calculated DIC and alkalinity

Table 7. PCO_2 measurements not used in calculations

Table 8. Land resource regions of the U.S., the pH is on the far right (Holmgren 1993)

Table 9. Properties and nutrients of soils classified in 1974 by FAO/UNESCO [Sillanpää, 1982 #18]

Table 10. (Within the text, page 31) Error estimation for parameters

Table 11. Total carbon flux in each Holdridge life-zone calculate from PCO_2 regression

Table 12. Flux from regressions with PCO_2, and from the average DIC for unknown life-zones

Table 13. Global flux and error bounds for different methods

Table 14. Total global flux result: summary

Abstract

In this research, the global annual flux of inorganic carbon into groundwater was calculated to be 4.4 GtC/y, with a lower bound of 1.4 GtC/y and an upper bound of 27.5 GtC/y. Starting with 44 soil PCO_2 measurements, the dissolved inorganic carbon (DIC) of the groundwater was determined by equilibrium equations for the carbonate system. The calculated DIC was then multiplied by the groundwater recharge to determine the annual carbon flux per area. These PCO_2 estimates were assigned to specific biotemperatures and precipitations according to the Holdridge life-zone classification system, and regressions between PCO_2, biotemperature, and precipitation were used to provide estimates for regions of the world that lacked PCO_2 measurements. The fluxes were mapped on a generalized Holdridge life-zone map, and the total flux for each life-zone was found by multiplying the calculated flux by the area in each life-zone. While there was a wide range in the error, the calculations in this study strongly suggest that the flux of carbon into groundwater is comparable to many of the major fluxes that have been tabulated for the carbon cycle.

The large flux that was calculated in this study was due to the high PCO_2 that is common in soils. The elevated PCO_2 levels are due to the decomposition of organic matter in soils, and the absorption of oxygen by plant roots. After the groundwater enters into rivers, it is possible that large amounts of CO_2 is released from the surface of rives, as the carbon-rich waters re-equilibrate with the low atmospheric PCO_2.

Introduction

CO_2 is the most abundant of the "greenhouse gases," and ice core records show that in the last 100 years, CO_2 concentrations in the atmosphere have been 40 percent higher than they were in the past 18,000 years. In order to understand what the human role has been in changing the atmospheric concentrations of CO_2, it is necessary to understand the carbon cycle. While many of the human additions to the carbon cycle have been well-documented, researchers have been unable to account for a significant fraction of the anthropogenic carbon. In this research the amount of CO_2 that enters into groundwater has been calculated for the entire Earth's land surface. Since this amount has never been calculated on a global scale, this study gives new results for a piece of the carbon cycle that has been overlooked or considered inconsequential.

There are many intermediate steps involved in transferring carbon from the atmosphere to groundwater (**Figure 1**), including photosynthesis and decomposition of organic matter. Due to these biological processes in the ground, the partial pressure of CO_2 (PCO_2) in soils is often 10 times higher than the PCO_2 in the atmosphere. The slow diffusion rate of CO_2 out of the ground keeps the PCO_2 high in the soil, and this pressure increases with depth.

In this study, calculations were made for how much CO_2 dissolves into the groundwater for particular areas. For these calculations, the values of CO_2 partial pressures in soils were taken from previous studies, and the amount of CO_2dissolved in the groundwater was found by applying chemical equilibrium equations. The flux of carbon into groundwater for a particular area was then obtained by multiplying the calculated concentration of CO_2 by a published rate of groundwater recharge for that area. The fluxes were then assigned to regions on a worldwide map of Holdridge life-zones, and for life-zones where there was not any PCO_2 data, regressions with temperature and

precipitation were used to assign PCO_2 estimates. Fluxes for these unknown life-zones were then computed in the same way as the fluxes for the known PCO_2 values.

The results from this study were displayed on a world map that shows the global distribution in the carbon-flux that enters into the groundwater. The global annual sum for this flux was found to be 4.4 gigatons carbon per year (GtC/y), with error estimates giving this value a lower limit of 1.4 GtC/y and an upper bound of 27.5 GtC/y. The magnitude of these results suggests that the flux of carbon into groundwater could have a substantial role in the global carbon cycle.

II. Background

Global Climate Change

In publications since the late 1980's, the Intergovernmental Panel on Climate Change (IPCC) has analyzed a wide array of factors that could lead to global climate change. The greenhouse gases, gases that absorb long-wavelength radiation in the atmosphere, are CO_2, CO_4, CFC's, N_2O, and No_x. If we can quantify the increase in concentration of greenhouse gases, we can calculate how much more long-wavelength radiation is being absorbed by the atmosphere. Measurements of greenhouse gases have been made at locations around the world, and these measurements can be compared to the various fluxes in the carbon cycle. By tabulating the human contribution to the greenhouse gases in the atmosphere, IPCC researchers have found numerical values for the degree to which people have contributed to the process of global warming.

The IPCC reports refer to the places that supply carbon to the atmosphere as "sources," and the destinations for carbon leaving the atmosphere as "sinks." "Reservoirs" are places that hold carbon, such as the atmosphere, soil or the ocean, and "fluxes" are the transfer rates between reservoirs. The components of the carbon cycle, including the anthropogenic sources, are shown in **Figure 2**. The largest global fluxes of carbon is the ocean involve the ocean and the ocean has been found to be a net sink for atmospheric carbon of about 2 GtC/y. Land plants provide the next largest fluxes of carbon since they absorb large quantities of CO_2 from the air through the process of photosynthesis. Land plants are held accountable for a net sink of about 1.4 GtC/y. Human activities that provide sources of atmospheric carbon include the burning of fossil fuel, slash-and-burn agriculture, and other farming practices. The IPCC reports detail the amount that each of these human activities has contributed carbon to the atmosphere, and provide estimates how much of this carbon could leave the atmosphere to various carbon

sinks. Researchers found that their measurements of the concentration of carbon in the atmosphere were different than the predicted values from previously studied carbon sinks. When they made this comparison, they found that there was 1.4 +/- 1.5 GtC less than they calculated (Houghton 1995). Hence, carbon was leaving the atmosphere to a sink (or many sinks) not considered in the IPCC's calculation.

One should note that **Figure 3** leaves out what have been considered to be small parts of the carbon cycle such as groundwater and river water. The inorganic carbon flux from rivers into the ocean, has been published as .3 GtC/y, and the organic carbon flux from rivers into oceans as .4 GtC/y (Suchet 1995). Suchet and Probst calculated that the flux of inorganic carbon from soils into groundwater. Eventually, the carbon from groundwater could make its way into oceans via rivers, be stored below ground in the form of carbonate minerals, or be released from rivers into the atmosphere.

The problem of the "missing sink" remains unsolved. According to the IPCC (Houghton 1995), likely solutions to the missing sink problem include: forest re-growth in the northern hemisphere, increased productivity in plants due to higher concentrations of CO_2 in the atmosphere, and higher plant productivity due to the deposition of nitrogen from human pollution. If we do not know where the missing carbon is going, it will be very difficult to make important decisions in a wide array of policy areas such as agriculture and energy usage. We need to understand every aspect of the carbon cycle and how well carbon sinks can absorb the human-derived greenhouse gases.

Dissolution of CO_2 into water

For carbon dioxide to move from the air to the water, it first dissolves into the aqueous form of CO_2. The dissolved CO_2 then interacts with the other ions in the water.

If there is enough time for these interactions to equilibrate, then the concentrations of the various ions in the water are related by several equilibrium reactions:

CO_2 (gas) <--> CO_2 (aq)	$K_h = \frac{[CO_2(aq)]}{PCO_2}$	(1)
CO_2(aq) + H_2O (l) <--> H^+(aq)+ HCO_3^-(aq)	$K_1 = \frac{[H^+][HCO_3^-]}{[CO_2(aq)]}$	(2)
HCO_3^-(aq) <--> H^+(aq) + CO_3^{2-}(aq)	$K_2 = \frac{[H^+][CO_3^{2-}]}{[HCO_3^-]}$	(3)

The brackets symbolize aqueous concentration, and PCO_2 is the partial pressure of CO_2 at the air-water boundary. The PCO_2 of a gas in air can be expressed in atmospheres as a fraction of the total atmospheric pressure, or as a volume-fraction of the air. In the equations above, the K's are the equilibrium coefficients and equation (1) is known as Henry's Law. These K's have a temperature dependence that have been determined through experiments and tabulated by researchers such as Plummer and Busenberg (1982).

Several details can be noted about these equations: First, the component that is written as, "CO_2 (aq)," is actually as combination of CO_2 (aq) and H_2CO_3 (aq), since these two species are difficult to distinguish. The term, "PCO_2," is actually an approximation for the fugacity, or "fCO_2," at the air-water boundary, or the amount of CO_2 that interacts with the water. The fugacity is the partial pressure multiplied by an extra factor, or "fugacity coefficient," that takes into consideration the non-ideal nature of the gases in the air. Since the fugacity coefficients are so close to one (**Figure 3**), PCO_2 was

considered equal to the fugacity for the purposes of this study. Lastly, the "activity," rather than the concentration of each species is what affects the reactions, although for most applications, the activity essentially equals the concentration. Seawater, for instance, has an activity of approximately 0.98, whereas freshwater's activity is nearly one (Drever 1997).

The reactions above describe the open carbonate system, in which water is in contact with air and the various constituents have enough time to equilibrate. The water that was equilibrated with air may migrate below the water table, closing it off from contact with air. Then, the other carbonate species will no longer be affected by Henry's law (equation 1), and new equilibrium concentrations will be reached among the carbonate species in the water. However, the total amount of dissolved, inorganic carbon (DIC) will remain constant, and because of this, it is convenient then to express the amount of CO_2 in water as the sum of the concentrations of these ions:

$$[DIC] = [CO_2(aq)] + [HCO_3^-(aq)] + [CO_3^{2-}(aq)] \quad (4)$$

Provided that the equilibrium coefficients are known, PCO_2 is known, and the pH of the water is known, the DIC can be found from the first three equations above. If the pH is not known, additional equations are needed to determine the value of $[H^+]$. The first additional expression is the dissociation of water:

$$H_2O \text{ <--> } H^+ + OH^- \quad K_w = [H^+][OH^-] \quad (5)$$

In addition to the total dissolved CO_2, another important conservative property in water is alkalinity. Alkalinity is a measure of how sensitive the pH of a solution is to changes in dissolved ion concentration. It can be measured through titration methods, and can also be derived from an expression of charge balance between the positively or negatively charged ions in the soil water:

$$[Na^+] + 2[Mg^{2+}] + 2[Ca^{2+}] + [H^+] + [\text{other cations}]$$
$$= [Cl^-]\ 2+[SO4^{2-}] + [HCO_3^-] + 2[CO_3^{2-}] + [OH^-] + [\text{other anions}] \quad (6)$$

This equation of charge balance can be rearranged so all of the ions that are strongly affected by pH are on one side of the equation, and this expression is defined as the alkalinity:

$$\text{Alkalinity} = [HCO_3^-] + 2[CO_3^{2-}] + [OH^-] + [\text{other weak anions}]$$
$$- [H^+] - [\text{other weak cations}] \quad (7)$$

The expression for alkalinity or the expression for charge balance can be combined with the equation (5) to derive the value of $[H^+]$, which can then be entered into the equilibrium expression for the reactions involving the carbonate ions. After this algebraic manipulation, the total dissolved CO_2 can be found as a function of the known parameters.

Soils

Soils have many ecological roles, including being a medium for plants to grow in, recycling nutrients and waste, providing a habitat for soil organisms, filtering rain water,

as well as providing the raw material used for farming and construction (Brady 1996). Soils decompose living carbon through microbial decomposition, transforming the carbon from its organic form as solid or dissolved organic matter. The way that soils transfer carbon between organic matter and the atmosphere has been the subject of many carbon-cycle models including the model by van Breeman and others (van Breemen 1990). Soil characteristics that have played a role in these studies include soil texture, temperature, decomposition rates, soil moisture, and time-variations.

What comprises a soil? Soil is defined as the "unconsolidated mineral or organic material at the surface of the earth capable of supporting plant growth," or "the stuff in which plants grow" (Bridges 1997). Liquid and gas components fill the pore space between soil particles, and below a critical depth, the water table, all of the pore space is composed of water. In addition, soils are characterized by soil "horizons," which are layers in the soil that have distinct appearances, textures, and chemical attributes. **Figure 4** portrays a picture of a soil profile, with soil horizons labeled as "A," "B," and "C" horizons. These three general horizon types are differentiated as: A) organic rich, B) containing accumulations of minerals, and C) below the root zone, and primarily consisting of weathered bedrock.

Plant and animal materials are decomposed by microorganisms in soils, releasing CO_2, as well as other gases. In addition, plants absorb oxygen, which increase the fraction of air which is CO_2 (the PCO_2). The gases in the soil then slowly mix with the atmosphere through the process of diffusion.

Soil water is sorbed onto clays and other the solid particles, and this water, as well as dissolved ions in the water can be extracted from soil particles by the suction of plant roots. The chemical properties of soils center around the transfer of ions between the soil water (or soil "solution") and to the surfaces of soil solids. Clay minerals, which

comprise a large fraction of the solid particles in a soil, have negatively charged surfaces, and attract the positively charged cations in the soil solution. The quantity of cations that can be bound to the clay minerals, and other soil solids, is called the "cation-exchange capacity," and this quantity depends on the type of clay minerals, and the amount of organic matter in the soil. The particles in soils are weathering products of the soil's "parent material," or bedrock, and have varying cation capacities. Depending on the type of environment, as well as the time that elapses in the weathering process, different clay minerals, and mineral oxides will form in the soil (**Figure 5**). In addition to clay minerals and mineral oxides, organic colloids that have negatively charged segments can also bind cations in the soil solution.

The pH of a soil solution, or the "soil's pH" is determined by the constituents of the soil solution, as well as by the PCO_2 of the soil gas. The cations that lead to an increase in pH are called "base-cations," and the most predominant of these are Ca^{2+} and Mg^{2+}, followed by K^+ and Na^+. With the addition of these base cations, the alkalinity of the soil solution increases, which buffers the solution from changes in pH. In addition to base cations, "acid-cations" decrease the alkalinity, and tend to lower the pH. The most prominent acid cation is H^+, followed by Al^{3+}. The ratio of acid to base-cations, rather than the cation-exchange capacity determines the buffering capacity of the soil solution, and controls the pH in the soil.

Since a soil's pH is determined largely by the type of cations in the soil solution, it is reasonable to expect that different geographic regions would have different chemical constituencies, and thus have different pH measurements in the soil. Indeed, this is the case, and soil surveys both in the United States and around the world have collected large databases for the nutrients in soils as well as the pH for individual soils (**Table 1** contains U. S. soil classification orders and the average pH in each soil order). In

addition to geographic differences, there are small pH differences between soil horizons at a particular place, due to varying clay constituents and organic matter of the soil profile. The geographic differences in pH fall under three general descriptions: 1) In warm, humid climates, the pH tends to be very low because all of the base-cations have been weathered out of the soil. As shown on the right side of **Figure 5**, the highly-weathered parent material leaves only iron and aluminum-oxides, which are composed of predominantly acid-cations. 2) In desert and semi-arid areas, the rapid evaporation of water leaves the soil solution concentrated in base cations such as sodium and calcium, which raises the pH. 3) Finally, in cold, wet places, the decomposition of organic matter occurs at a very slow rate, which leaves the soil solution rich with organic acids, which lowers the pH.

The classification systems used by the Food and Agricultural Organization of the United Nations (FAO) and by the United States Soil Survey share the characteristic that group soils according to diagnostic soil horizons. The soil classifications are structured like biological taxonomic levels, with the highest soil type being the order, followed by suborder, group, and soil series. While there are a few differences, the FAO and the United States soil classifications are very similar, with the FAO having a few more soil orders than the U. S. system, and slightly different names.

Groundwater Recharge

The hydrosphere has many distinct components, the largest of which is the ocean (96.5%), glaciers (1.74%), and groundwater (1.7%). The remaining water of the hydrosphere is contained in lakes, rivers, and the atmosphere (Shiklomanov 1983). In order to know the rate of water exchange between different components of the

hydrosphere, several equations involving different fluxes need to be solved simultaneously. One representation of these equations is (L'vovich 1979):

$$P = S + R_g + E \quad (8)$$

$$R_{tot} = S + R_g \quad (9)$$

$$W = P - S = R_g + E \quad (10)$$

$$K_U = Rg / W \quad (11)$$

$$K_E = E / W = 1 - K_E \quad (12)$$

$$E = f(P,E_{max}) = E_{max} * \tanh(P/ E_{max}) \quad (13)$$

Here, the fluxes of water (in units of volume per area) are: precipitation (P), wetting of the ground (W), evapotranspiration (E, the sum of evaporation and transpiration by plants), total runoff (R_{tot}), groundwater runoff (R_g), and surface runoff (S). There are two dimensionless parameters in these equations, the groundwater runoff coefficient (K_U) and the evapotranspiration coefficient (K_E).

In order to make a map of groundwater recharge worldwide, L'vovich started with measurements of precipitation and total runoff into rivers, and solved for all the other parameters from the above equations. Equation 13) is the most complicated of these equations and is a curve-fit to data. The errors in this interpolation curve range between 2 to 18 percent from measured data taken from different parts of the world. The coefficients K_U and K_E derive from other hydrologic computations, and may contain additional errors. After solving these equations for 71 different segments of the Earth's land surface, L'vovich displayed his calculated amounts for groundwater recharge on a world map, half of which is shown in **Figure 6**.

Holdridge Life-zones:

The Holdridge life-zones, shown in **Figure 7**, correlate environmental parameters with vegetation regions (Holdridge 1972). The two parameters of precipitation and biotemperature determine a location's classification in the Holdridge scheme. The temperature regions are represented as the horizontal rows in the triangular figure, and are named as latitudinal belts ranging from "polar" to "subtropical," an these same regions are classified according to altitudinal descriptions. The third axis of the triangle in **Figure 8** is the Potential evapotranspiration ratio (PETR), and is calculated as a function of temperature and precipitation. Life- zones that share the same PETR are labeled as humidity provinces, and range from "semi-parched" to "superhumid." A horizontal dashed line is drawn between the warm-temperate and subtropical temperature regions, separating the life-zones that are prone to frost from the frost-free zones at the bottom of the diagram.

Instead of temperature, or mean annual temperature, the Holdridge life-zone classification uses the quantity, "biotemperature." Based on the assumption that plants grow most favorably in temperatures ranging from 0 to 30^0 C, biotemperature is computed by summing the monthly temperatures between 0 and 30^0 C, then dividing by 12. By defining temperature in this way, places that have high mean annual temperatures actually have slightly lower biotemperatures, and cold places have slightly higher temperatures. In order to bypass the need to collect monthly temperatures, Holdridge published an empirical relation between biotemperature, mean annual temperature and latitude, that applies for mean annual temperatures above 24^0 C (Holdridge 1972):

$$\text{Biotemp} = T - (3/100)\, L\, (T - 24) \qquad (14)$$

Where T is the mean annual temperature in ^{0}C and L is the latitude in degrees. This relationship is shown in **Figure 9** as a contour plot, where the x and y axes are Temp and Latitude and contours of biotemperature are shown as curves on this diagram. One can see from **Figure 9** that above 24^{0}C, biotemperature decreases with increasing temperatures, presumably due to greater seasonal fluctuations of temperature at higher latitudes.

Originally , Holdridge (Holdridge 1947) developed the life-zone system as a way of distinguishing forest types in the tropics, and extended the classification system to the rest of the world. Since the Holdridge life-zones predict vegetation type and climatic conditions, this classification scheme provides an excellent way to relate carbon-cycle data to different terrestrial ecosystems (Kirschenbaum 1996). As an example of a way that the Holdridge classification scheme has been incorporated into carbon-cycle research, Post and others (Post 1982) published their results for the carbon and nitrogen storage held in each life zone, as well as the areas for each of the life-zones.

There are several other classification schemes that predict vegetation types from climatic and hydrologic parameters such as evapotranspiration, temperature, and precipitation. Prentice (Prentice 1992) compared four of these classifications in terms of their ability to predict the vegetation in the land areas for each of these classification schemes, and the classifications differed slightly in terms of the vegetation that they predicted. More recently, Holdridge life-zones have been found to be poor in describing differences in Seasonality (Leeman 1999). Despite its flaws, the Holdridge system was used in this study because of the way in which the Holdridge life-zones are grouped according to temperature and precipitation, and because of the limited accuracy of the calculations.

Methods Summary

The calculations in this study can be summarized by a single equation. The basic equation used in calculating the flux of carbon (per unit area) into groundwater was:

$$\left[\frac{Flux}{Area}\right] = R_g \cdot PCO_2 \cdot K_h \cdot \left(1 + \frac{K_1}{10^{-pH}} + \frac{K_1 K_2}{10^{-2pH}}\right) \qquad (15)$$

In this equation, the parameters on the right include the PCO_2, the pH, the groundwater recharge (R_g), and the equilibrium constants (K_1, K_2, and K_h). The part of equation (15) to the right of "R_g" is the equilibrium DIC for a particular location. This part of the equation was determined by the equilibrium chemistry equations, and chosen because the parameters involved could be estimated. The equilibrium DIC was then multiplied by R_g to give the flux per area.

The starting point for this research was PCO_2 data for soils around the world. Brook and others (Brook 1983) collected PCO_2 data from many sources, and published a world map of soil PCO_2 based on regressions with evapotranspiration. This study was done in the same fashion, and includes much of the PCO_2 data published by Brook and others. **Table 2** shows the PCO_2 measurements with their sources and locations, and these locations are shown on a map in **Figure 10**. The complete set of parameters used in the study is shown in **Table 3**. Since the equilibrium constants can be determined from empirical relationships with temperature (Plummer 1982), mean annual temperature data was collected from published sources. After the parameters used in equation (15) were compiled, error estimates were made for each of the parameters involved estimates was used to calculate the error in the results.

While equation (15) gave the carbon flux per unit area for each of the PCO_2 localities, it was necessary to multiply these fluxes by areas to determine the total global

carbon flux. Because of the sparseness of PCO_2 data around the world (**Figure 10**), regressions that involved climatic information was used to correlate regions of the world that shared similar climates but were separated by large distances. The known PCO_2 data was regressed against biotemperature and precipitation in order to estimate PCO_2 for regions of the world without PCO_2 data. These regressions were used to determine PCO_2 values for 23 of the 38 Holdridge life-zones, and with PCO_2 values for all of the Holdridge life-zones, equation (15) gave the total carbon flux for each life-zone. Finally, the total fluxes for each life-zone were summed to give the global flux.

Chemistry of Carbonate System

The goal of using the equilibrium chemistry equations was to determine the amount of dissolved inorganic carbon from the PCO_2 data and from other parameters. The total dissolved inorganic carbon (DIC) in groundwater was found by solving a system of simultaneous equations described above. There are several possible ways to tackle this problem, and the method chosen depends on which of the parameters are known. One of the key assumptions was that the carbonate reactions dominate the equilibrium concentrations of the carbonate species (Butler 1982). Examples of additional reactions that could affect the carbonate system include reactions involving calcium ions (Ca^{2+}), organic compounds, as well as various reactions involving the dissolution of minerals in the soil or bedrock. These assumptions were tested by comparing empirical measurements to calculations.

If the pH and the PCO_2 is known, the DIC can be found by combining the three equilibrium equations for the carbonate system. It follows from the three carbonate equations (1,2, and 3) that:

$$[DIC] = K_h(PCO_2)\left(1 + \frac{K_1}{[H^+]} + \frac{K_2 K_1}{[H^+]^2}\right) \qquad (16)$$

In order to use this last expression to find DIC, it is necessary that one knows Kh, PCO_2 and $[H^+]$. $[H^+]$ is found from the pH as 10^{-pH}.

Alternatively, one could use an expression for the alkalinity to arrive at a value for DIC, forgoing any measured or assumed value for the pH. To do this, first K_w is expressed as:

$$K_w = [H^+][OH^-] \tag{5}$$

Then, continuing with the assumption that the carbonate reactions dominate the equilibrium conditions (Butler 1982), the alkalinity is then defined as:

$$Alk = [HCO_3^-] + 2[CO_2(\text{aq})] + [OH^-] - [H^+] \tag{17}$$

Using equation (16), the Alkalinity is then:

$$Alk = K_h(PCO_2)\left(\frac{K_1}{[H^+]} + \frac{2K_1K_2}{[H^+]^2}\right) + \frac{K_w}{[H^+]} - [H^+] \tag{18}$$

Then, this expression can be approximated as:

$$Alk \approx \frac{K_hK_1(PCO_2)}{[H^+]} - [H^+] \tag{19}$$

This approximation is tested in **Table 4**, where the terms, $(K_1K_2/[H^+]^2)$ and $(K_w/[H^+])$, are shown to be negligible compared to the other terms, for a realistic range of pH and temperatures.

Equations (5) and (19) are then two equations with four variables: Alk, PCO_2, $[H^+]$, and DIC. $[H^+]$ is found by taking the negative log of the pH. The K's are considered constants, and can be found from empirical relations with temperature (Plummer 1982). If any two of these four variables are known, the others can be calculated by solving these two equations simultaneously. There are then three possible

ways to determine DIC from the other variables, and these methods are summarized in **Table 5** below. In addition to a combination of the three parameters, PCO_2, pH, and alkalinity, each of these methods also requires an additional parameter, temperature (T) in order to determine the equilibrium constants:

Table 5. Three ways to calculate DIC

Method 1: Start with PCO_2, [H+], and T:

$$[DIC] = K_h(PCO_2)\left(1 + \frac{K_1}{[H^+]} + \frac{K_2 K_1}{[H^+]^2}\right) \tag{16}$$

Method 2: Start with alkalinity (Alk), [H+], and T:

$$[DIC] = \left(Alk + [H^+]\right)\left(\frac{[H^+]}{K_1}\right)\left(1 + \frac{K_1}{[H^+]} + \frac{K_1 K_2}{[H^+]^2}\right) \tag{20}$$

Method 3: Start with PCO_2, alkalinity (Alk), and T:

$$[DIC] = K_h(PCO_2)\cdot\left[1 + \frac{2K_1}{\left(-Alk + \sqrt{(Alk)^2 + 4K_h K_1(PCO_2)}\right)} + \frac{4K_1 K_2}{\left(-Alk + \sqrt{(Alk)^2 + 4K_h K_1(PCO_2)}\right)^2}\right] \tag{21}$$

In order to choose one of these methods, it was necessary to examine which of the variables were known. It turns out that there is little data about the alkalinity of groundwater or soils. However, the pH of soils has been well documented for a multitude of soil types that have been mapped world-wide. For this reason, method 1 was chosen over methods 2 and 3. If there was a way to estimate a soil's alkalinity based

on its geographic location, method 2 or method 3 could be used to calculate both the PCO_2 in the soil and the dissolved inorganic carbon. If this were the case, method 2 could be used to add information where PCO_2 measurements are not available.

An important part of determining which method to use was to estimate the sensitivity of the calculations to the parameters PCO_2,T, and pH. The variation of the equilibrium constants with temperature was taken from empirical results by Plummer and Busenberg (Plummer 1982):

$$\log(K_h) = 108.3865 + .01985076T - \frac{6919.53}{T} - 40.45154\log(T) + \frac{669365}{T^2} \qquad (22)$$

$$\log(K_1) = -356.3094 - .06091964T + \frac{21834.37}{T} + 126.8339\log(T) - \frac{1684915}{T^2} \qquad (23)$$

$$\log(K_2) = -107.8871 - .03252849T + \frac{5151.79}{T} + 38.92561\log(T) - \frac{563713.9}{T^2} \qquad (24)$$

Figures. 11-13 show how these constants vary between 0^0 and 30^0 C. The decrease of K_h and subsequent increase of DIC at higher temperature is due to the fact that the dissolved CO_2 transforms more readily to a gas at higher temperatures. To see how both pH and temperature affect the DIC values, **Figure 14** shows DIC values as contours, for a constant PCO_2 of .005 atm. One can see from this figure that for a given temperature, DIC is not sensitive to changes in pH until the pH increases to about 5 or 5.5. For example, with T=280 Kelvin (7^0 C), the DIC is constant at 0.25 mmol/kg between pH=3 to pH=5. Then, from pH=5 to pH=7.5, there is a tenfold increase in DIC from 0.25 mmol/kg to 2.5 mmol/kg.

In order to test whether it is a valid assumption to ignore any additional reactions besides carbonate reactions (1), (2), and (3), it was necessary to find a published source that included more than two of the relevant parameters: pH, alkalinity, DIC, and PCO_2.

Table 6 shows the results of these calculations from two different sources. In each of these cases, the calculated values were fairly closed to their measured values.

One can see from equation (16) above (method 1), that the dissociation of CO_2 in water increases the amount of CO_2 that would dissolve from what one would calculate with only Henry's Law. If only Henry's law is used,

$$[DIC] = K_h(PCO_2). \tag{25}$$

By using the other two equilibrium reactions (2,3), this amount increases by the factor:

$$\left(1 + \frac{K_1}{[H^+]} + \frac{K_2 K_1}{[H^+]^2}\right). \tag{26}$$

The extra amount of dissolved inorganic carbon is due to the reactions that CO_2 undergoes in the aqueous phase. As CO_2 reacts with water to form $HCO3^-$ and $CO3^{2-}$, the aqueous CO_2, on right side of the reaction described by Henry's law diminishes, and more CO_2 dissolves until equilibrium is reached. Regardless of the chemistry in the water, the dissociation if CO_2 into other dissolved ions increases the DIC from the value one would calculate by purely using Henry's law. In order to produce a lower bound for DIC, Henry's Law, which only depends on PCO_2 and temperature, was used as a comparison to the results that were obtained by using PCO_2, pH and temperature (method 1 above).

Data Gathering Methods

PCO_2:

The PCO_2 data originated from a variety of published sources, and in total, 44 PCO_2 values were used in the calculations (**Table 2** and **Figure 10**). Wherever possible, the annual averages of PCO_2 were used as data for this study, as well as the PCO_2 measurements closest to the water table.

Some of the data was set aside at the beginning of the analysis and these fell into two categories: PCO_2 measurements taken in carbonate areas, and a group of measurements from an area with coal and lignite (**Table 7**). The reason that PCO_2 from areas with carbonate bedrock were set aside was that calcium (Ca^{2+}) and calcium carbonate ($CaCO_3$) affect the equilibrium conditions in the carbonate system. Only a small percentage of the world contains carbonate bedrock, and furthermore, coal and other petroleum deposits comprise only a small fraction of the world's bedrock, and were ignored in these calculations.

Researchers have collected PCO_2 data for a variety of purposes, including microbial activity in soils (Hendry 1993); soil formation in carbonate terrain (Reardon 1979); chemical evolution of groundwater in glacial terrain (Wallick 1981); and still others have measured PCO_2 in conjunction with isotopic studies to trace the origin of CO_2 in soils (Cerling 1991). In none of the papers used in this study, were PCO_2 measurements compiled for the purpose of calculating the flux of carbon into the groundwater.

A large amount of the PCO_2 data is from North America, there is some from Europe, Australia, Amazon forests in South America, but very little from Africa and large

parts of Asia (**Figure 10**). The geographic deficiency of the published PCO_2 data is due to a lack of field studies in many parts of the world.

In many field studies, researchers have demonstrated the seasonality of soil PCO_2. If a given paper included data showing the change of PCO_2 over time, an average was taken of the published data, either by eyeballing the average from a graph of the time-evolution of soil PCO_2, or by averaging a set of numbers included in the published paper.

pH estimation:

A pH estimate was made for those locations whose PCO_2 sources did not include the pH of the soil or groundwater Depending on the location in the world for such a PCO_2 measurement, this estimate was made in different ways.

For different regions in the U.S., **Figure 15** shows the average pH (Holmgren 1993). In the article that this figure is published, Holmgren and others also included a table for the pH values for 9 soil orders (**Table 1**) in the U.S. soil classification system, as well as a pH averages for different "land resource regions" in the U.S. (**Figure 16** and **Table 8**).

For locations outside the U. S., the FAO soil maps (FAO/UNESCO 1974) were used to determine soil types. Then, the pH was found from **Table 9** (Sillanpää 1982). In order to convert from $pH(CaCl_2)$ to $pH(H_2O)$, Silanpää provides the empirical formula:

$$pH(H_2O) = 0.937 + 0.934\ pH(CaCl_2) \qquad (27)$$

In the cases where the FAO maps were too detailed for the purpose of this study, a generalized soil map of the world in order to make a rough estimate of the soil type was used (**Figure 17**). Since many of the FAO soil classification units have changed since

1974, it was necessary to compare the descriptions for each of the soil orders in Bridges (Bridges 1997) and in the World Soil Reference Base (FAO/UNESCO 1974). In addition, a world soil map with U.S. soil orders was used to estimate the pH of Holdridge Life-zones (**Figure 18**).

Climate and hydrologic parameters

For temperature and precipitation data, there were several sources in addition to the sources for PCO_2. These included Korzoun (Korzoun 1977) and L'vovitch (L'vovich 1979). For temperature data, the mean annual temperature was taken from these sources. The biotemperature, which is used in the Holdridge life-zone calculations, is found using the monthly mean temperatures, as discussed in the **Background** section above. For locations with biotemperatures above 24^0 C, equation (4) was used to convert the mean annual temperature to biotemperature. For places with mean annual temperatures less than 10 ^{0}C, the biotemperature was computed by averaging the monthly mean temperatures and using zero for the months with temperatures below 0^0 C. None of these colder regions, however, had a biotemperature that differed by more than 0.5^0 C from the mean annual temperature.

Whereas the biotemperatures were used to determine the Holdridge life-zones, the mean annual temperatures were used in the calculations for DIC. Seasonal fluctuations in temperature were ignored because at the water table, the temperature does not fluctuate nearly as much as at the surface.

The recharge of groundwater was found from the map in L'vovitch (L'vovich 1979) (**Figure 6**). Since many researchers now believe that most of the total runoff is actually mostly groundwater runoff rather than a combination of both groundwater *and*

surface runoff, calculations were made with total runoff (R_{tot}), in addition to the groundwater runoff (R_g).

Error in parameters

In order to compute the error in the calculations, estimates were made for the errors in the data gathering techniques, as summarized in the table below:

Table 10

Parameter	Error
PCO_2	50% of PCO_2
pH	1
Precip.	10% of Precip
Rg	25% of R_g
Rtot	25% of R_{tot}
Mean Annual Temp.	3^0C

The reason that some of these errors are in the form of a percentage is that the method used to obtain these parameters was largely guesswork. For instance, when looking at the groundwater recharge map in **Figure 6**, it is clear that there is a lot of variation in R_g. However, for places with high and low R_g, one can see a local variation in the contours of about 25%. (The contours on the map were described by L'vovitch as having an error between 2 and 18%). For obtaining PCO_2 measurements, graphs showing yearly fluctuations were eyeballed, and leading to a high margin of error, hence the 50% error estimate shown above.

Regressions

For the life-zones that had PCO_2 data, the carbon flux was found using equation (15). In order to make the calculations for the unknown life-zones, pH and recharge values were assigned to each life zone by using soil and hydrologic maps. Then, it was possible to estimate the carbon flux into groundwater by extending regression curves from the life-zones with known PCO_2 measurements. PCO_2 was estimated from the regression curves according to the temperature and precipitation located at the centers of the Holdridge life-zones (**Figure 8**).

The independent variables in the regressions were precipitation (Precip) and biotemperature (Biotemp), and for each regression, there was one dependent variable, $\log(PCO_2)$. Because PCO_2 ranged over several orders of magnitudes, $\log(PCO_2)$ was used instead PCO_2, making the regressions semi-logarithmic instead of purely linear regressions. These regressions were then compared to the PCO_2 regressions from Brook and others (Brook 1983).

The regressions were made using the least squares method, in which the coefficients were found for a linear relationship between the dependent and independent variables. For the regressions made with between one dependent and one independent variable, such as between PCO_2 and temperature, the regression curve could be plotted as a straight line. For regressions with two independent variables, such as between $\log(PCO_2)$ and both biotemperature and precipitation, the regression produced a plane in the 3-dimensional space by the three parameters.

Since the uncertainty of the known PCO_2 and DIC estimates was small compared to the variations between neighboring points, this uncertainty of the measurements was not used in calculating the uncertainty of the regression curves. Instead, 95% confidence values for the coefficients of the linear fits were used to make rough estimates for the

upper and lower bounds of the results. For the upper bound estimations, the uppermost value of each of the parameters was used in to determine the carbon-fluxes for the known Holdridge life-zones. One exception was temperature, in which the upper temperature limit was used to calculate the lower limit of the DIC, and the lower limit was used to calculate the upper limit of the DIC. For the unknown life-zones, the uppermost coefficients for the 95% confidence interval were used. One possible statistical method that may be used in further calculations is a Monte Carlo simulation, which would help determine the error more precisely. Matlab numerical software provided the regression functions used in these calculations.

In order to further explore the possible bounds of for the calculations in this study, the PCO_2 regressions were repeated with three different approaches to the chemistry and the hydrologic data. The primary calculation was based on the carbonate chemistry involving all three of the carbonate reactions, equations 1,2, and 3, in the **Background** section above, and the groundwater recharge. The groundwater recharge, from L'vovitch and others (L'vovich 1979), may significantly underestimate the actual water than infiltrates into the ground, so the calculations with "total recharge" give results that are much larger than those made with groundwater recharge. Finally, the calculations made with groundwater recharge and "K_h only" were made using the simplest process for the dissolution of CO_2 into water, Henry's law.

Depth Correction

One additional method that was considered for this study was to estimate the PCO_2 at the water table based on a PCO_2 measurement higher in the soil profile. Although this method was not used in the calculations, it is possible that future calculations could involve the correction for depth which is described below.

Because of the slow diffusion rate of CO_2, the air within the soil tends to have a much higher PCO_2 than the atmosphere. However, as is indicated in **Figure 1**, the diffusion of CO_2 upward and out of the soil causes the PCO_2 to decrease towards the surface. Many of the papers that have PCO_2 measurements include graphs of PCO_2 as a function of depth, and some show PCO_2 as a function of both depth and time (**Figures 19-21**). A simple model for diffusion of CO_2 through the soil was used to derive an expression for the PCO_2 at the water table. In this derivation, only the steady state profile of CO_2 was considered, since the parameters used in this study are yearly averages.

The diffusion equation used in this derivation is known as Fick's law, and can be expressed as:

$$\frac{\partial C}{\partial z} = d_{fick} \cdot C(z) \qquad (28)$$

Here, z is depth, C is PCO_2, and d_{fick} is the diffusion coefficient. In addition to diffusion the soil was assumed to have a source of CO_2 (microbial decomposition of organic matter) spread evenly throughout the soil profile. The boundary conditions for soil PCO_2 were that the concentration was equal to the atmospheric value ($10^{-3.5}$ atm) at the soil surface, and for there to be a no-flow boundary-condition at the water table. The derivation for the PCO_2 concentration in the soil profile is given in **Figure 22**, and **Figure 23** shows the PCO_2 as a function of depth.

For a given PCO_2 at a particular depth z_1 the PCO_2 at the water table was found to be:

$$C_D = \frac{D^2C_1 - D^2C_{at} - z_1^2C_{at} + 2z_1C_{at}D}{z_1(-z_1 + 2D)}, \tag{29}$$

where C_D is the PCO_2 at the water-table, D is the depth of the water table, C_{at} is the PCO_2 in the atmosphere, and z_1 is depth of the measured PCO_2 in the soil. This is the equation that could be used to extrapolate a PCO_2 measurement to give an estimate for the PCO_2 at the water table, and the necessary parameters are given this equation

The results of this simple model is supported by the published PCO_2 profiles for individual locations (**Figs. 19-21**), as well as by a composite plot of the data used in this model (**Figure 24**). Further, in **Figure 21**, one can see that the profiles are roughly parabolic in shape. Aberrations from this profile could be due to transient effects related to the growing season. For example, **Figure 19** shows PCO_2 decreasing with depth during the summer months, whereas after August, the PCO_2 profile in **Figure 19** returned to the steady-state in which PCO_2 increases with depth. In the composite plot, **Figure 24**, a linear fit between PCO_2 and depth is plotted to illustrate that PCO_2 increases with depth even for a wide range of locations.

The validity of the no-flow boundary condition can be illustrated by using the PCO_2 information from Brazil, shown as number 1 in **Table 3**. By assuming that the PCO_2 of .07 atm. is at the water table, the ideal gas law, PV=nRT, leads to a gas-concentration of .13 kg/m^3. With T=300 K, pH=5.8, the DIC is found from equation (16) to be .00294 mol/l. With a groundwater recharge of 200 mm/year, this then leads to a flux of CO_2 of .6 kg/m^2/year, which is $1.9*10^{-9}$ kg/m^2/s. In order to compare this flux of CO_2 into the groundwater to the flux of CO_2 towards the ground surface, one first needs to find the gradient of PCO_2 in the soil. For a first approximation, one can approximate this gradient as linear, with CO_2 concentration decreasing from the water table to the

atmosphere ($PCO_2=10^{-3.5}$). With the depth of the water table measured as 45 m, the gradient would then be:

$$\frac{\partial C}{\partial z} = \frac{.07 \text{ atm} - .003 \text{ atm}}{10 \text{ m}} = .0067 \text{ atm} \cdot \text{m}^{-1} \qquad (30)$$

With a diffusion coefficient of .144 cm^2/s (Thorstenson 1983), this leads to an upward diffusive flux of $1.7*10^{-7}$ $kg/m^2/s$, which is 100 times faster than the downward flux of CO_2 into the groundwater.

Unfortunately, very few of the papers with PCO_2 data included the depth of the water table. Rather than arbitrarily guessing what the depth of the water table for most of the PCO_2 measurements, this method was not used in the calculations. Since the PCO_2 measurements that were used mostly were taken at shallow depths, a correction for the depth of the water table would increase the PCO_2 used in equation (15), and increase the total global carbon flux calculated in this study.

Results

The results from these calculations show that the flux of carbon into groundwater is on the order of 5 GtC per year. The carbon flux per area are mapped in **Figure 25**, and the calculations for each Holdridge life-zone are shown in **Table 7**. The fluxes that were obtained by extending the PCO_2 regressions are labeled with an asterisk, and if there was more than one PCO_2 measurement in a life-zone, the resulting fluxes were averaged. The results shown in the map were made by using the PCO_2 regression for the unknown Holdridge life-zones. The final result for the total global flux was 4.4 GtC/year, with an upper bound of 27.5 and a lower bound of 1.4 GtC/year.

The regression that was used in making the map in **Figure 25** is shown as a contour graph in **Figure 26** In this figure, the contour lines represent the regressed values for PCO_2 from the two dependent variables, biotemperature and precipitation. The color-bar on the right provides a scale for the contour lines, as well as for the known PCO_2 values, plotted as stars. Since the precipitation and temperature parameters estimates were identical for many of the PCO_2 measurements, many of the known PCO_2's are at the same location on this map and on the contour plot. Because of this, **Figure 26** contains only 27 stars, whereas there were 44 PCO_2 measurements. The equation for the fit between log(PCO_2) and Biotemperature and precipitation was:

$$\text{Log}\,(PCO_2) = -2.62 + 0.0192(\text{Biotemp}) + 0.000277(\text{Precip}),\ R^2 = 0.29 \qquad (31)$$

where Biotemp is in ^{0}C and "Precip" is precipitation in mm/year. The small R^2 was due to the large spread in PCO_2 data. This low R^2 motivated an alternative calculation for the global carbon flux, in which the DIC values for the unknown life-zones were taken to be the average DIC that was calculated for the 44 PCO_2 measurements.

As a comparison to the regressions done by Brook and others (Brook 1983), regressions were made with temperature, instead of biotemperature. The results are shown in **Figures 27** and **28**, and one can see from these figures that the linear regressions were nearly identical to the regressions published by Brook and others. This is not a surprise, since nearly half of the PCO_2 measurements used in this study came from their 1983 paper. The fact that the R^2 values were significantly lower in this study can be attributed to the small amount of data both in this study and the study by Brook and others. Brook and others made their world soil-PCO_2 map based on another regression, with actual evapotranspiration (AET), which they found had a slightly higher R^2 when regressed against PCO_2. As a comparison to their study, further regressions may be done using the AET data, although it is not likely that the results would be very different.

In **Figure 29**, one can see the flux calculations for the 6 temperature regions in the Holdridge life-zone classification. Precipitation increases from left to right on this plot, as in the triangular diagram (**Figure 8**). One can see that the flux increases rapidly from the left into the middle, and then for the life-zones with the most precipitation on the right, the fluxes decrease slightly. This decrease is due to the lower pH values that exist in extremely wet climates. The soils in these climates contain a high percentage of iron and aluminum oxides, as well as a large amount of organic acids, making the pH comparatively low. In arid life-zones, on the left side of **Figure 29**, the fluxes are lower, but the error bounds are much larger. This is because of the high pH in arid soils and the greater sensitivity of the calculations at higher pH (**Figure 14**).

For each of the methods involving the carbonate chemistry and recharge values, two ways used to determine the flux for Holdridge life-zones that did not have any known PCO_2 data: PCO_2 regressions and taking the average DIC from all of the known

life-zones. **Tables 12 and 13** show the primary results for the regressions for PCO_2 and for averaged DIC. Whereas the PCO_2 regression gave a global flux of 4.4 GtC/y, result from using the average DIC to determine the DIC for unknown life-zone was 5.3 GtC/y. These two ways for calculating the flux in the unknown life-zones were repeated for the calculations involving the total recharge, and for simplest CO_2 dissolution reaction, Henry's law. For the pure-Henry's law calculation, the global flux was 3.2 GtC/y for the PCO_2 regression and 3.3 GtC/y for the DIC-averaging calculation. For the method using the total recharge and the three carbonate chemistry reactions, these values for the global flux were 13.7 GtC/year and 19.1 GtC/year. The results for these different methods, as well as estimates for the upper bounds and lower bounds for each calculation, are summarized below in **Tables 14**.

Discussion

The carbon flux calculated in this study is quite large, and is comparable to several of the major fluxes that have been established for the carbon cycle. For example, primary production on land is shown in **Figure 2** to be responsible for a flux of 61.4 GtC/y, respiration on land produces a flux of 60 GtC/y, and fossil fuel production as 5.5 GtC/y (Houghton 1995). The inorganic carbon flux from rivers into the ocean, has been published as .3 GtC/y, the organic carbon flux from rivers into oceans as .4 GtC/y (Suchet 1995).

There were several ways that the calculation of 4.4 GtC/year is bounded. Through the use of error estimates for the initial parameters, the lower bound for this primary calculation was 1.4 GtC/y. By using only Henry's law to calculate the DIC at the water table, neglecting any dissociation of CO_2 into other carbonate ions, the calculated carbon flux was 3.2 GtC/y, with a lower bound of 1.4 GtC/y. The lower bound calculations show that the flux of carbon into groundwater is a significant part of the carbon cycle. This conclusion is strengthened by the fact that the errors were calculated by using the extreme limits of all of the parameters to make the calculations of the upper and lower bounds. While there were errors in the estimates of pH, recharge and in the PCO_2 data, it is unlikely that the maximum of all of these errors occurred at the same time.

Where, then could 4.4 gigatons per year fit into the carbon cycle? One explanation for why people have overlooked this flux is that CO_2 is released into the air when the groundwater reaches a river. Any measurements for DIC in a river will be less than the DIC in the river's groundwater sources, due to the difference in soil PCO_2 and the atmospheric PCO_2 at the river's surface. Suchet and Probst (Suchet 1995) calculated the flux of carbon through chemical weathering of bedrock, and based their calculations

on measurement of the constituents bicarbonate (HCO_3^-) concentrations in river water. They assumed that bicarbonate in the rivers was at equilibrium with the river water, and the bicarbonate originated from the weathering reactions of bedrock.

The idea that rivers could be supersaturated with CO_2 due to groundwater inputs is discussed by Hope and others (1995). In addition, studies involving the Amazon River by Devol and others (Devol 1987) found an excess of dissolved CO_2 gas, and related this excess to emission of CO_2 from the surface of rivers. From their calculations, Devol and others found that for a 1,700 km stretch of the Amazon river, there was a CO_2 loss of 37.4 kmol/s to the atmosphere, or 0.14 GtC/year. Since this value does not include the CO_2 loss to the atmosphere in tributaries to the Amazon, it doesn't relate directly to the calculations in this study, which are based on recharge rates per area. Much of the CO_2 excess that were found in the Amazon River may also be due to biological activity in the river itself. The large flux of carbon from the Amazon River into the atmosphere could then be related to the flux of carbon that was calculated in this study.

One question that arises from this study is whether groundwater could be a sink for atmospheric carbon. While groundwater does not absorb atmospheric carbon directly, since the CO_2 at the water table is mainly derived from microbial decomposition in soils, an increase in atmospheric CO_2 would probably not result in an immediate increase in the flux of carbon into groundwater. If, however, there has been an increase of plant growth in some parts of the terrestrial biosphere (Houghton 1995), soil PCO_2 would increase as the new plant materials decay. It follows then, that the flux of carbon into groundwater would increase as well. In order to determine whether the ground below the water table is a significant sink within a given time-frame, it would be necessary to calculate the precise quantities for the different fluxes involved between groundwater, soil, the soil

air, and rivers. In addition, the fluxes of dissolved organic carbon (DOC) would need to be considered as well.

This study gave a range of estimates for one of the fluxes in the carbon cycle, rather than provide a definite number. To reach a more precise answer for the carbon flux, several techniques could be applied. First and foremost, the number of PCO_2 measurements would need to be vastly increased. The published measurements used in this study were obtained from made with many different instruments, and under widely varying conditions, and there only 44 datapoints used in the calculations. Also, a large number of the measurements were made at different parts of the year, and with different variations in time and space. In addition to more PCO_2 measurements, a fuller description of the chemical conditions of the groundwater at each location, including the pH and alkalinity, would contribute to more accurate calculations.

Conclusion

The global carbon flux of 4.4 GtC/y was derived from published PCO_2 data, annual temperature and precipitation data, as well as estimates for groundwater recharge. Since the flux calculated is quite high, and has been disregarded in most previous publications regarding the carbon cycle, conservative estimates were used wherever possible in these calculations. One example is that the PCO_2 measurements used in these calculations were mostly taken above the water table, while the PCO_2 closer to the water table is most likely higher. In addition the calculation only involving Henry's law gave an estimated total global flux of 3.2 GtC/y, and estimates for the lower bounds for these calculations gave a results above 1 GtC/y. Even with these conservative estimates, the total flux calculated was comparable to many of the major fluxes in the carbon cycle.

Because of the possibility for global warming to have a major impact on human lives and the biosphere in general, many researchers have been working to balance the large number of fluxes in the carbon cycle. It is uncertain where the carbon from spent fossil fuel goes after it enters the atmosphere, and recently, the terrestrial biosphere has been targeted as being a possible location for the "missing sink" in the global carbon cycle. While this study provides only a rough estimate for the flux of inorganic carbon into groundwater, it provides evidence that there could be other significant fluxes in the carbon cycle that have been overlooked. The results of these calculations show that the transport of carbon into groundwater could be an important part of future carbon-cycle research.

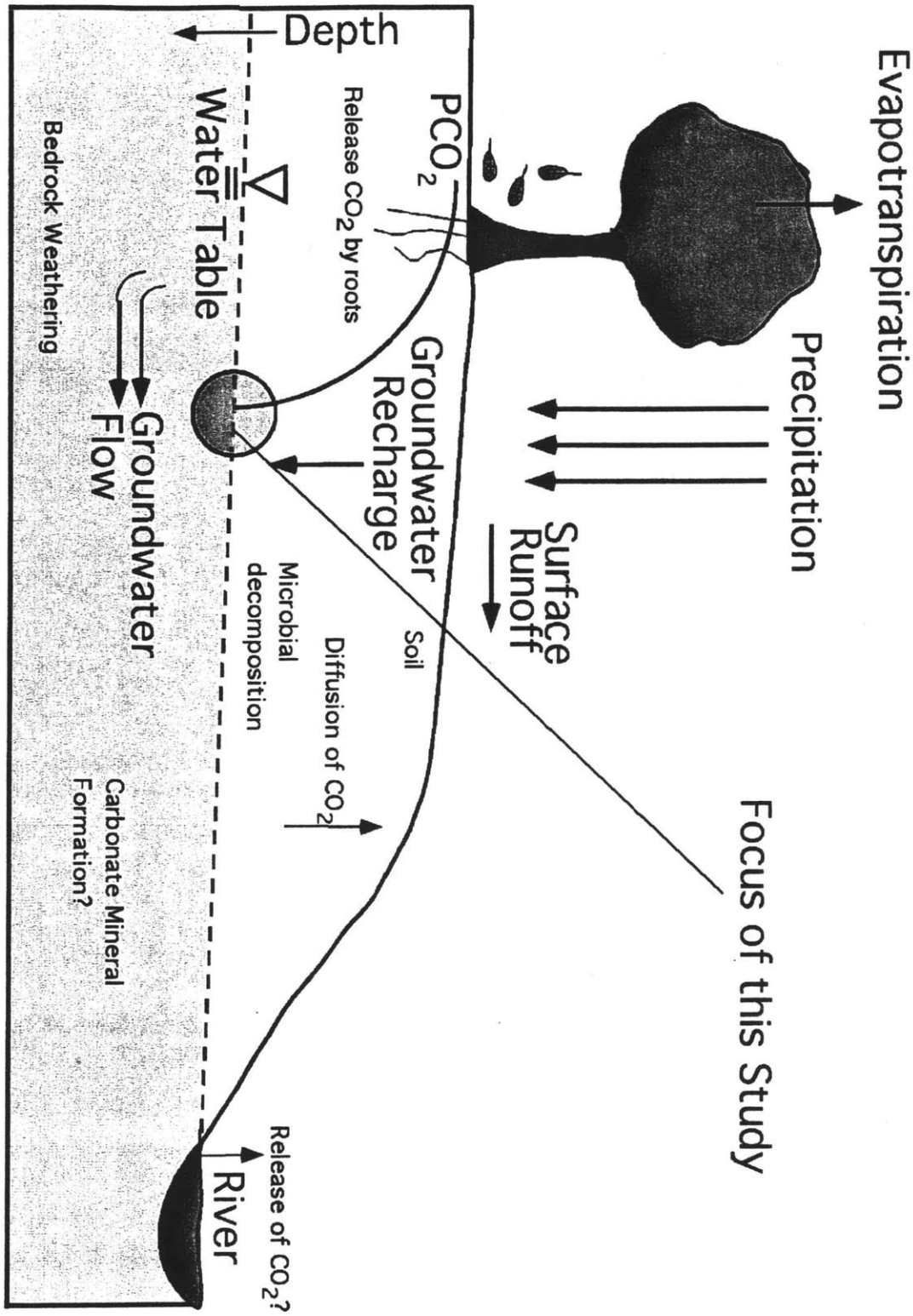

Figure 1. Diagram showing the path of CO_2 in the ground with the focus of this study at the water table.

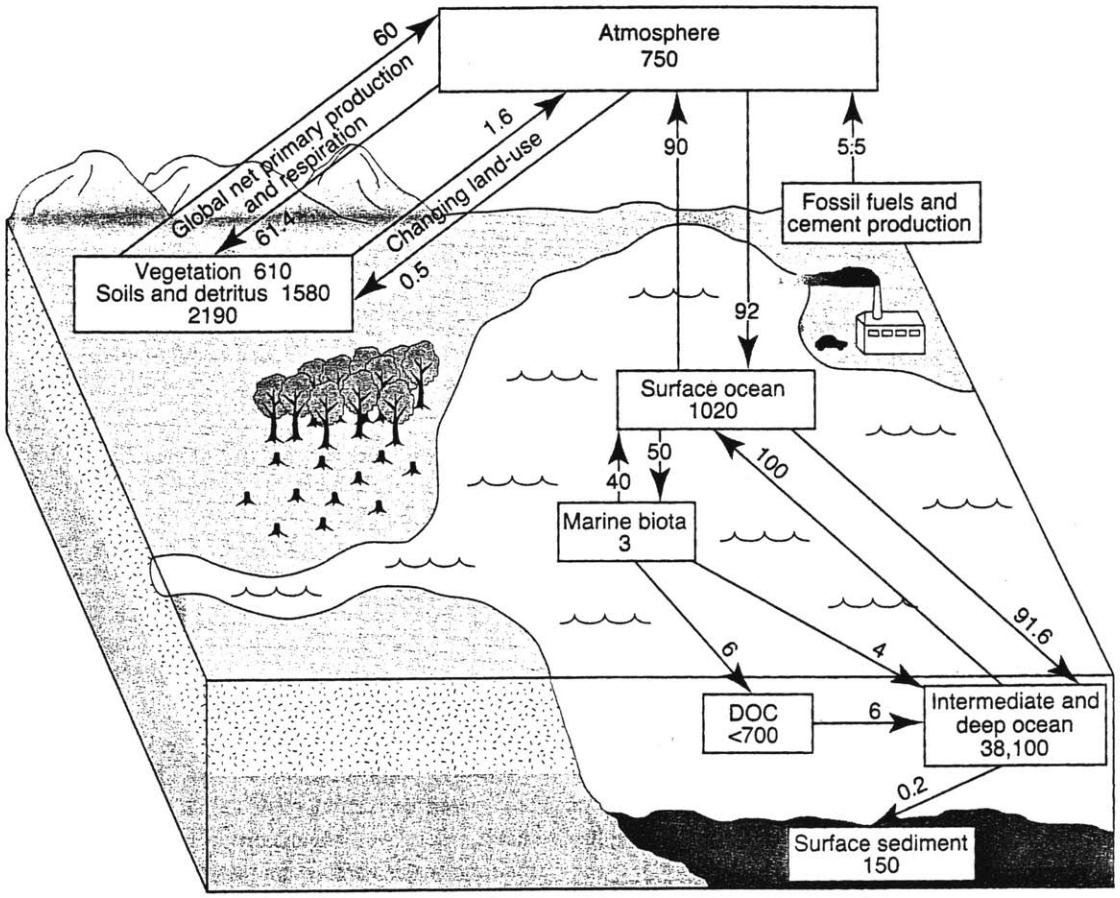

Figure 2. The global carbon cycle, showing the reservoirs in gigatons of carbon (GtC) and fluxes in GtC/y, as annual averages from 1980 to 1989. (Houghton 1995)

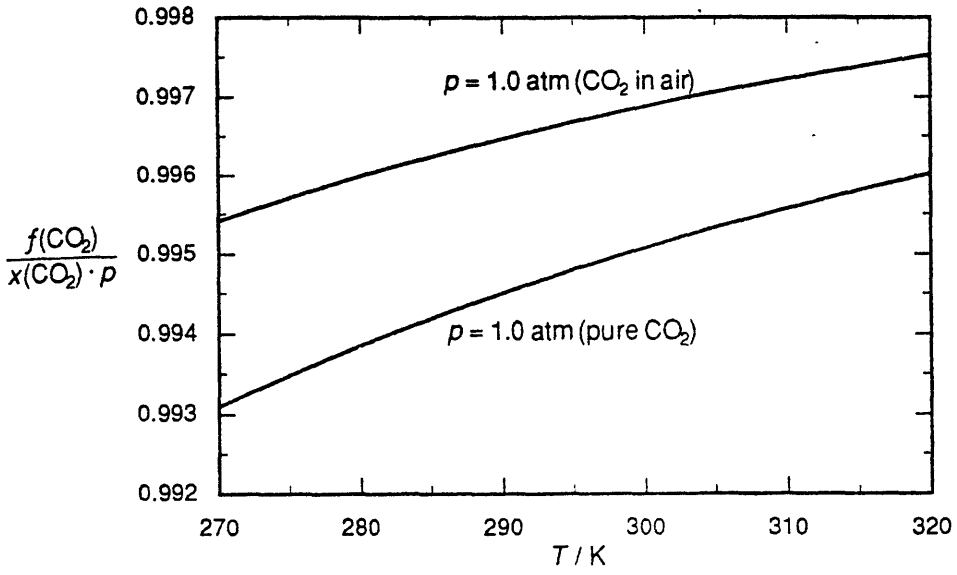

Figure 3. The ratio of fugacity (fCO_2) to PCO_2 between 270 and 320 Kelvin (DOE 1994)

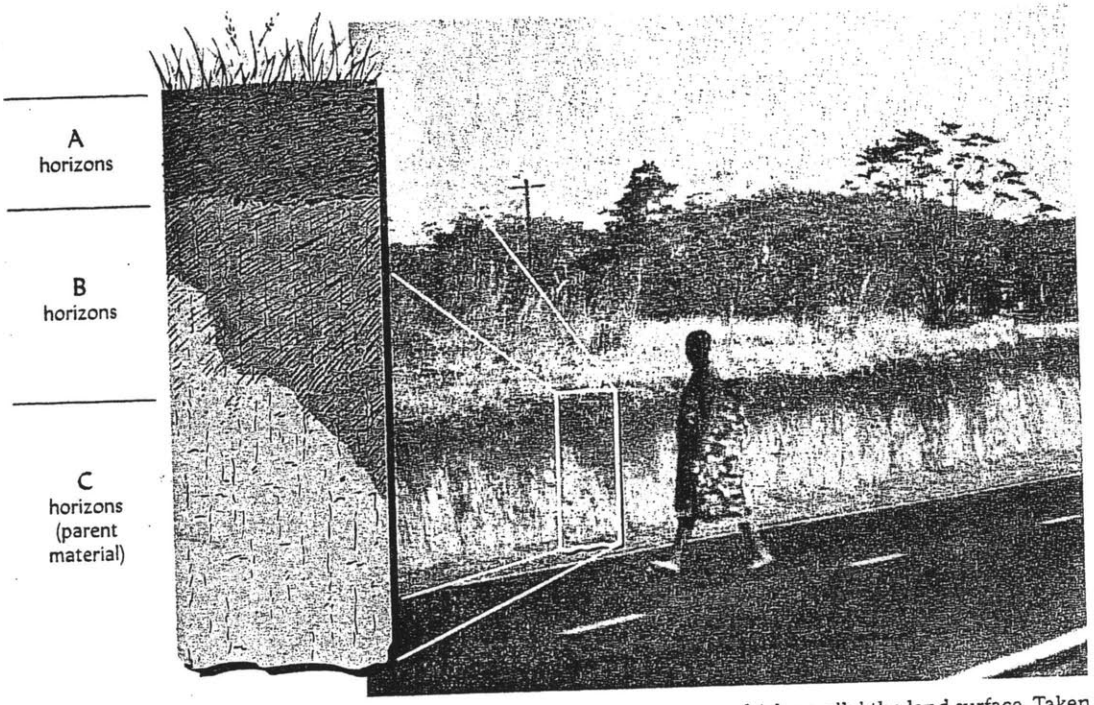

FIGURE 1.10 This road cut in central Africa reveals soil layers or horizons which parallel the land surface. Taken together, these horizons comprise the profile of this soil, as shown in the enlarged diagram. The upper horizons are designated *A horizons*. They are usually higher in organic matter and darker in color than the lower horizons. Some constituents, such as iron oxides and clays, have been moved downward from the A horizons by percolating rainwater. The lower horizon, called a *B horizon*, is sometimes a zone in which clays and iron oxides have accumulated, and in which distinctive structure has formed. The presence and characteristics of the horizons in this profile distinguish this soil from the thousands of other soils in the world. (Photo courtesy of R. Weil)

Figure 4. Soil horizons from a road cut in central Africa (Brady 1996)

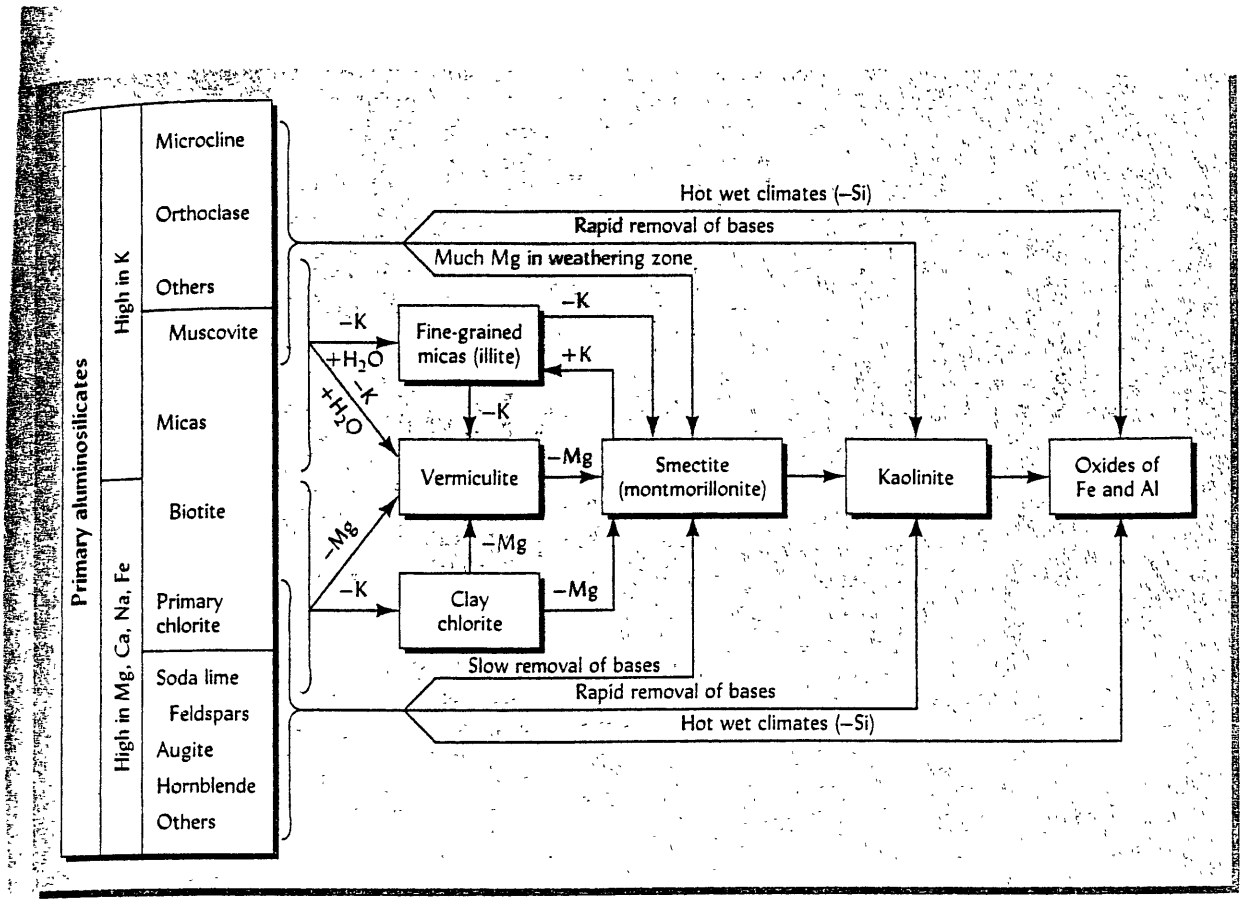

...General conditions for the formation of the various layer silicate clays and oxides of iron and aluminum. Fine-grained micas, chlorite, and vermiculite are formed through rather mild weathering of primary aluminosilicate minerals, whereas kaolinite and oxides of iron and aluminum are products of much more intense weathering. Conditions of intermediate weathering intensity encourage the formation of smectite. In each case silicate clay genesis is accompanied by the removal in solution of such elements as K, Na, Ca, and Mg.

Figure 5. The formation of clays and oxides of iron and aluminum by the weathering of bedrock.

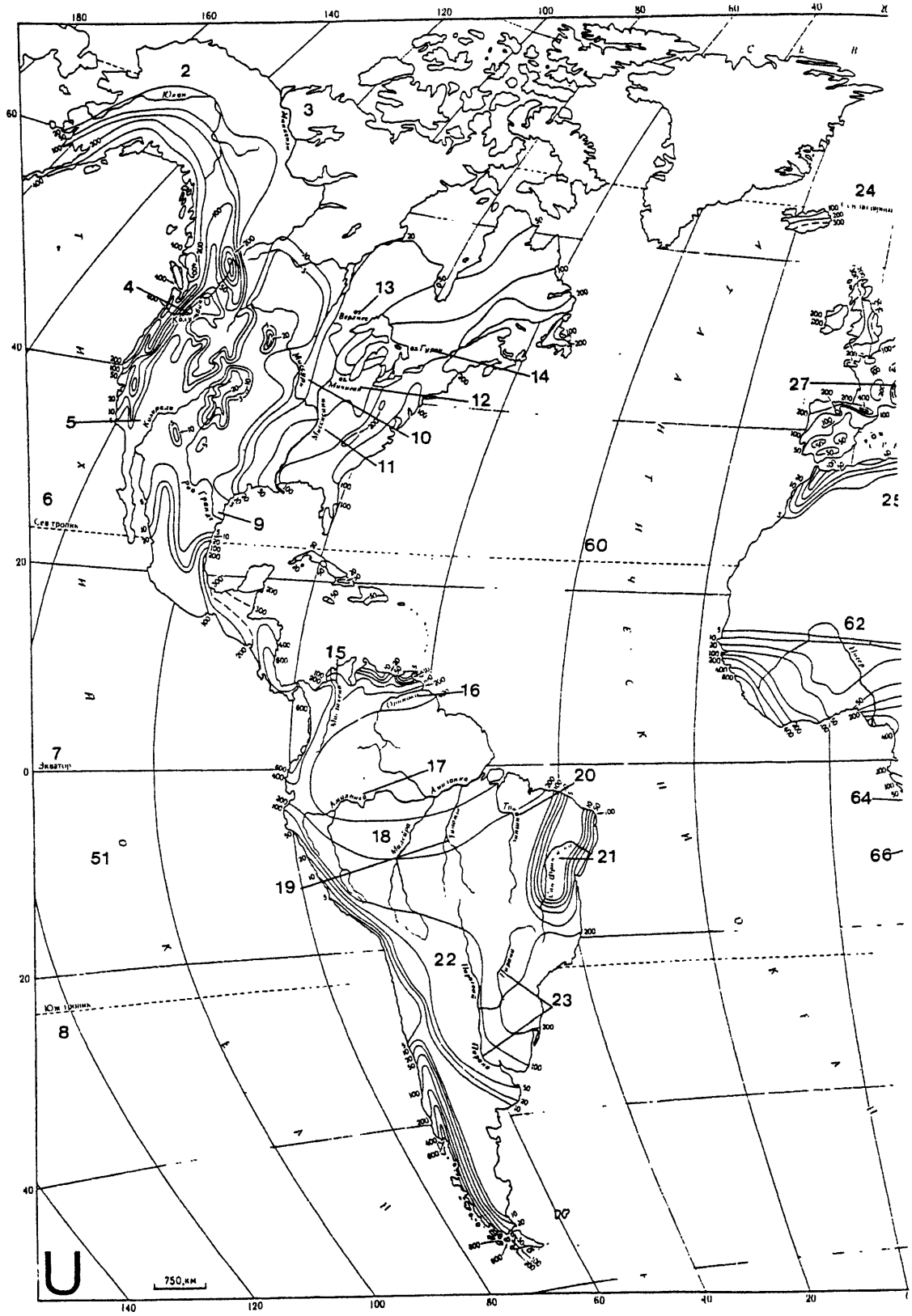

Figure 6. Groundwater recharge (R_g) for the Western Hemisphere. The larger numbers on the map are references to particular rivers, and the smaller numbers are R_g values in mm/y. The names on the map are in Russian, although the text of the book is translated. (L'vovich 1979)

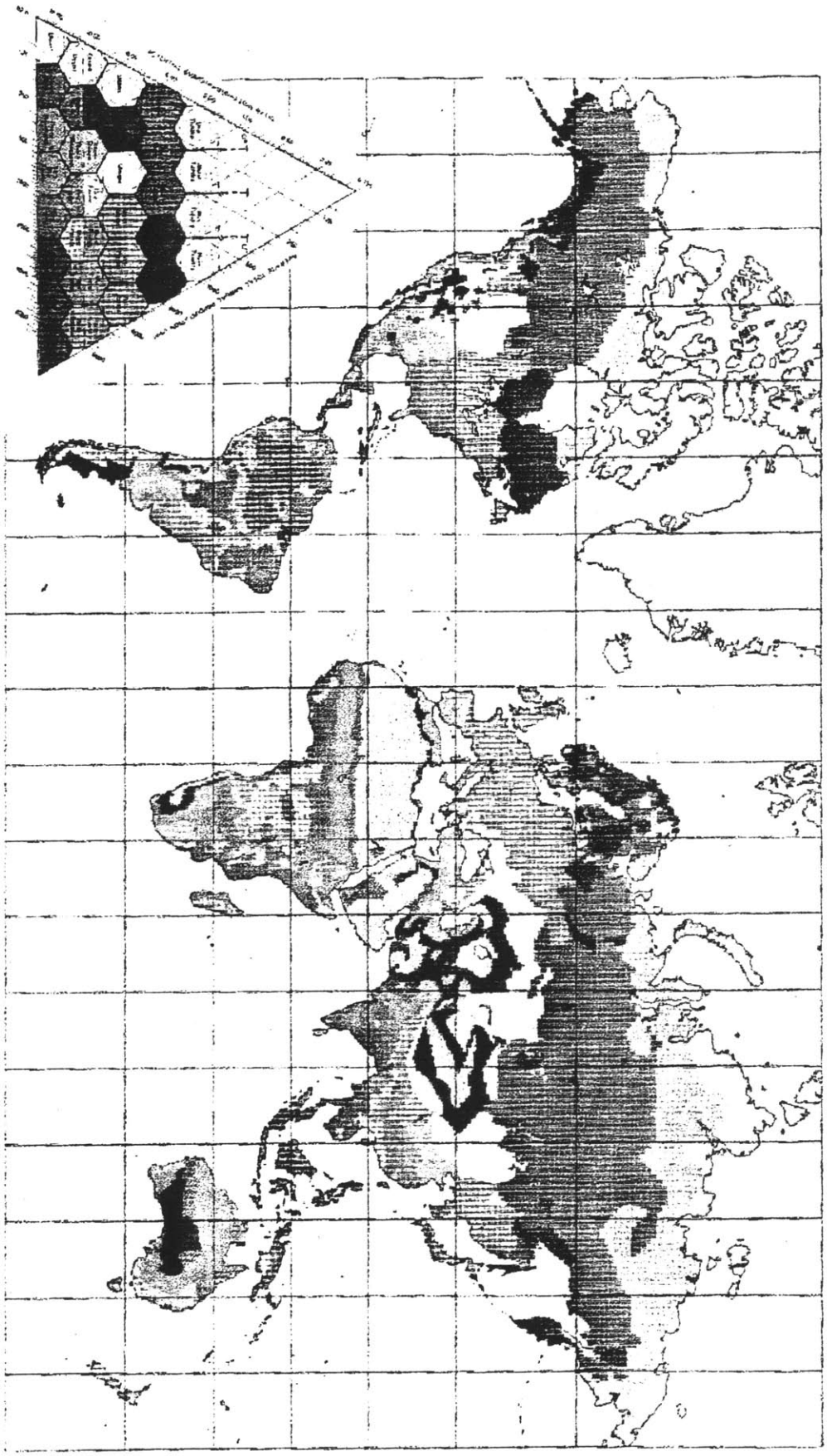

Figure 7. World map of the Holdridge life-zones (Emanuel 1985)

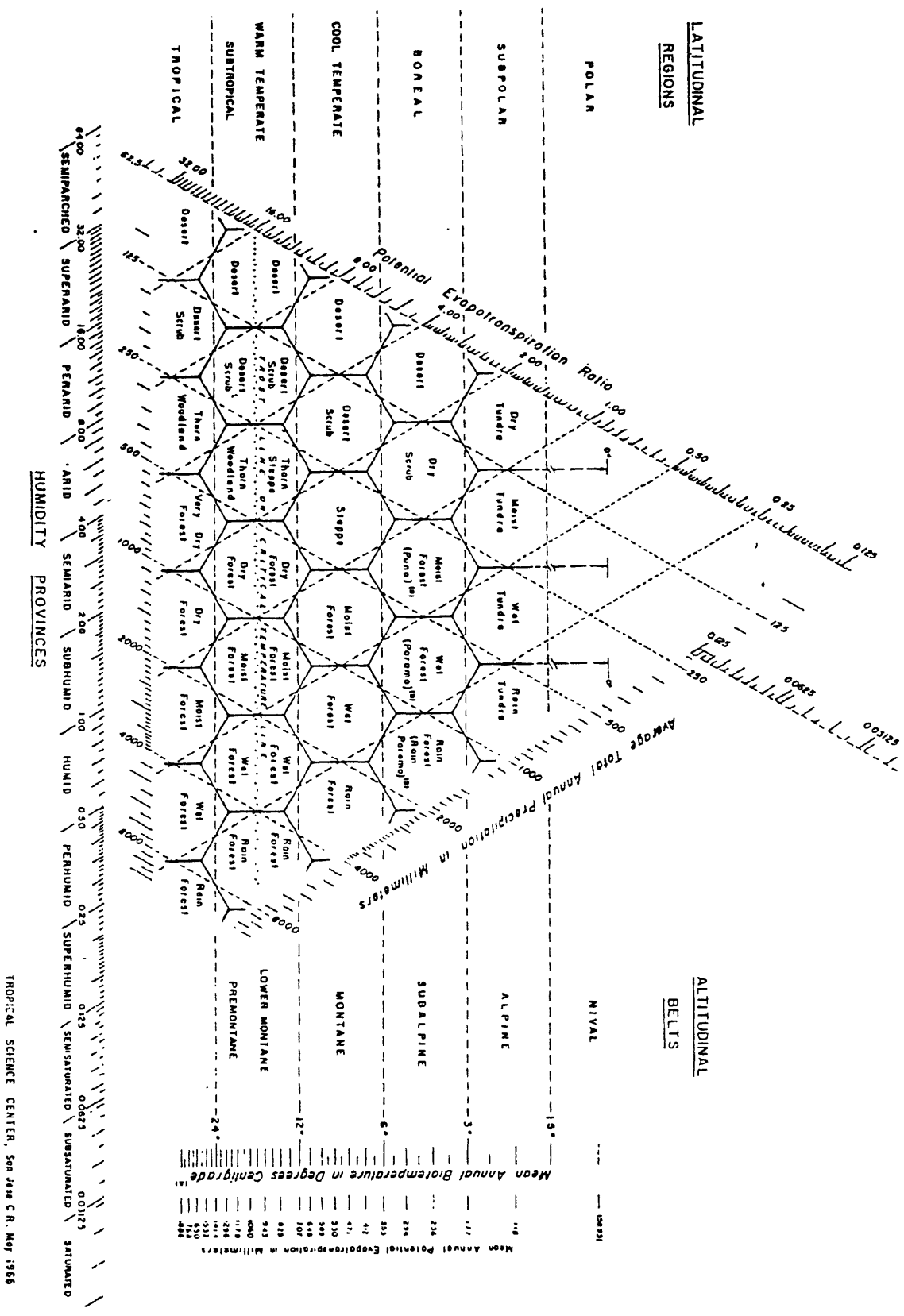

Figure 8. Classification scheme for the Holdridge life-zones. The vertical axis is temperature and the two diagonal axes are precipitation and potential evapotranspiration ratio. (Holdridge 1972)

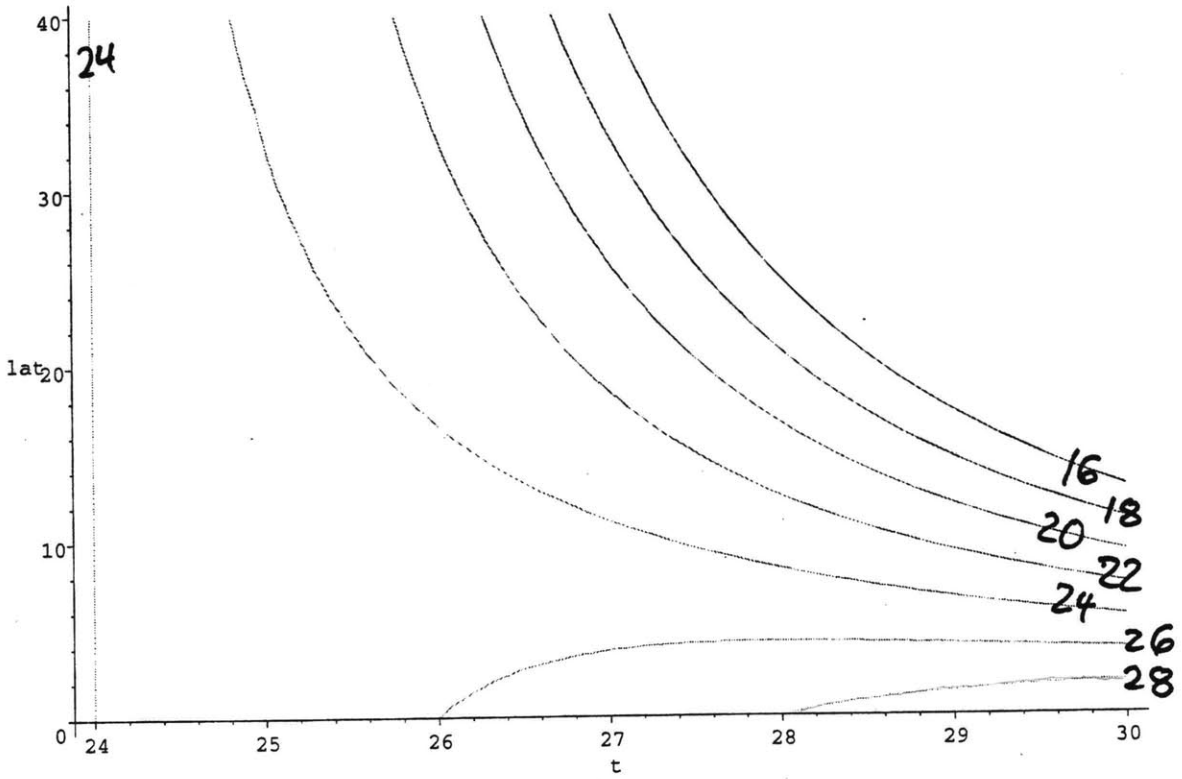

Figure 9. Biotemperature plotted as contours, as a function of temperature and latitude

Figure 10. Locations of PCO_2 measurements used in this study.

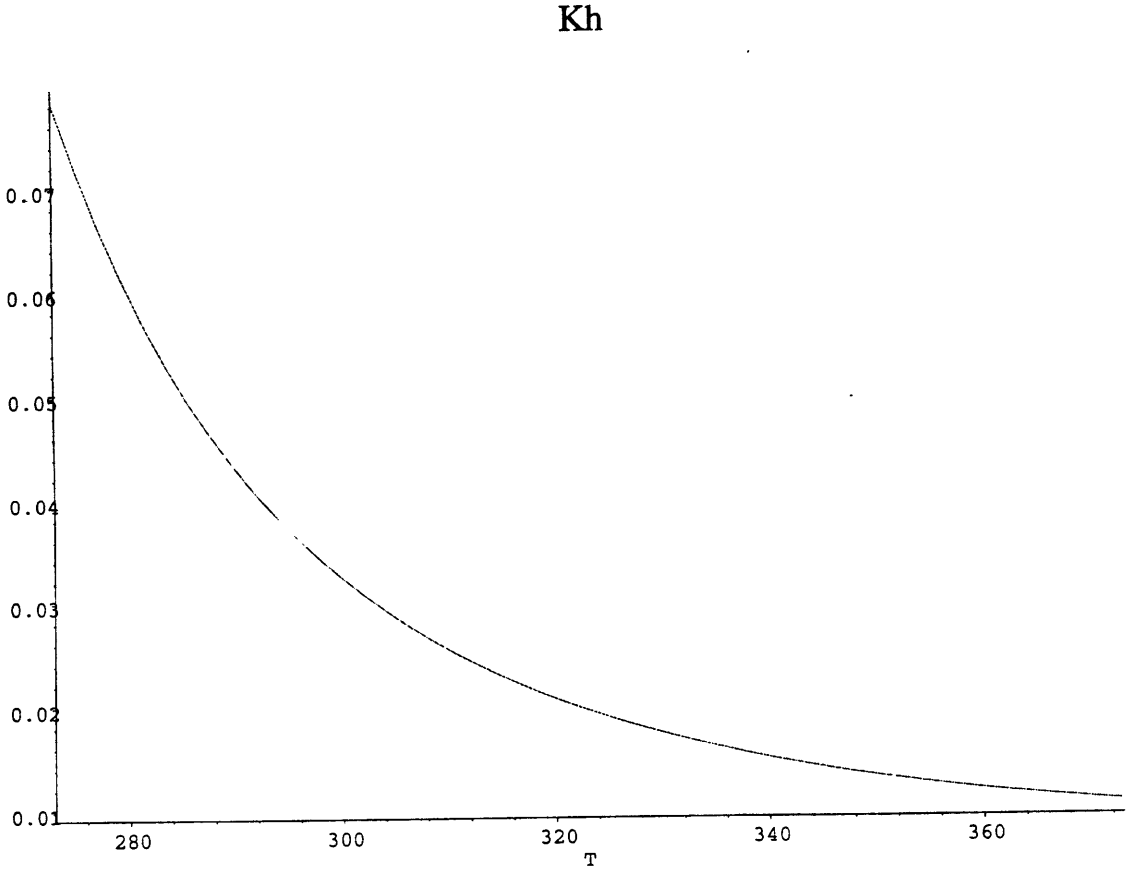

Figure 11. K_h as a function of temperature (Plummer 1982)

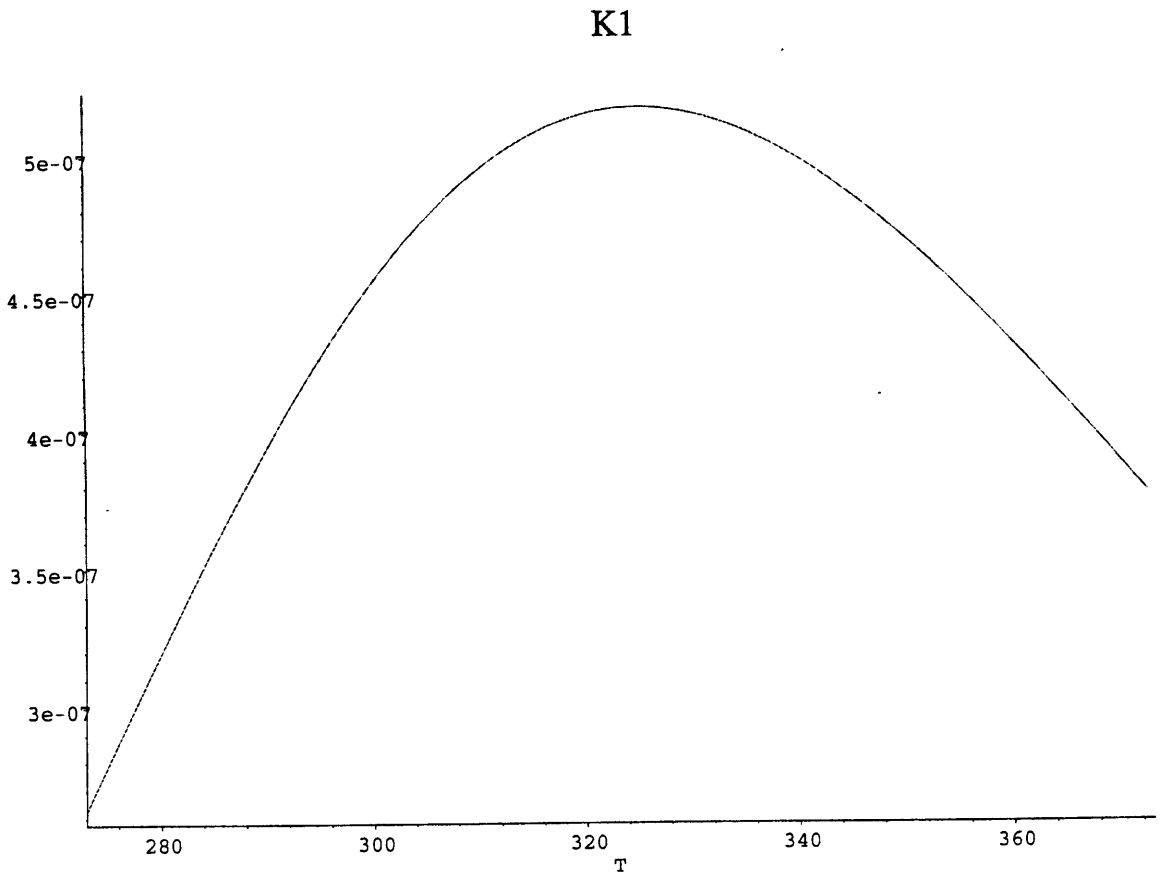

Figure 12. K_1 as a function of temperature (Plummer 1982)

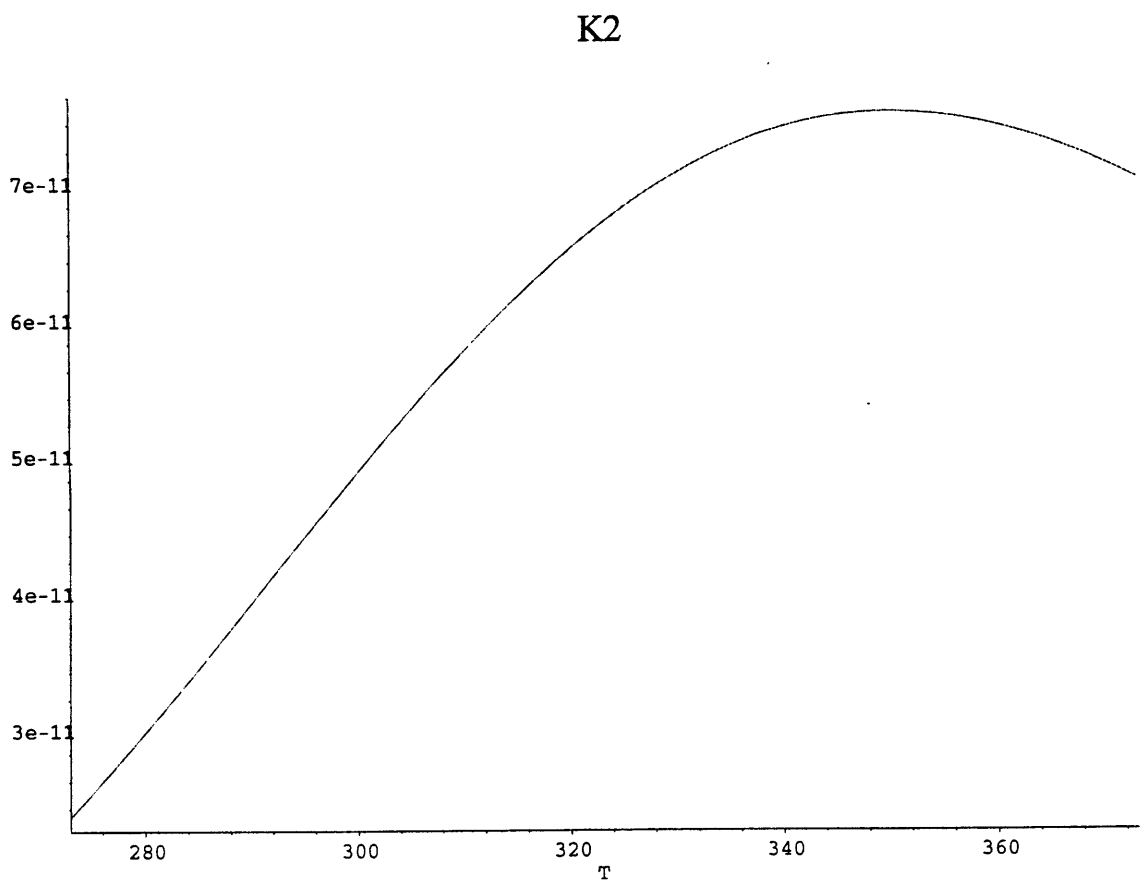

Figure 13. K_2 as a function of temperature (Plummer 1982)

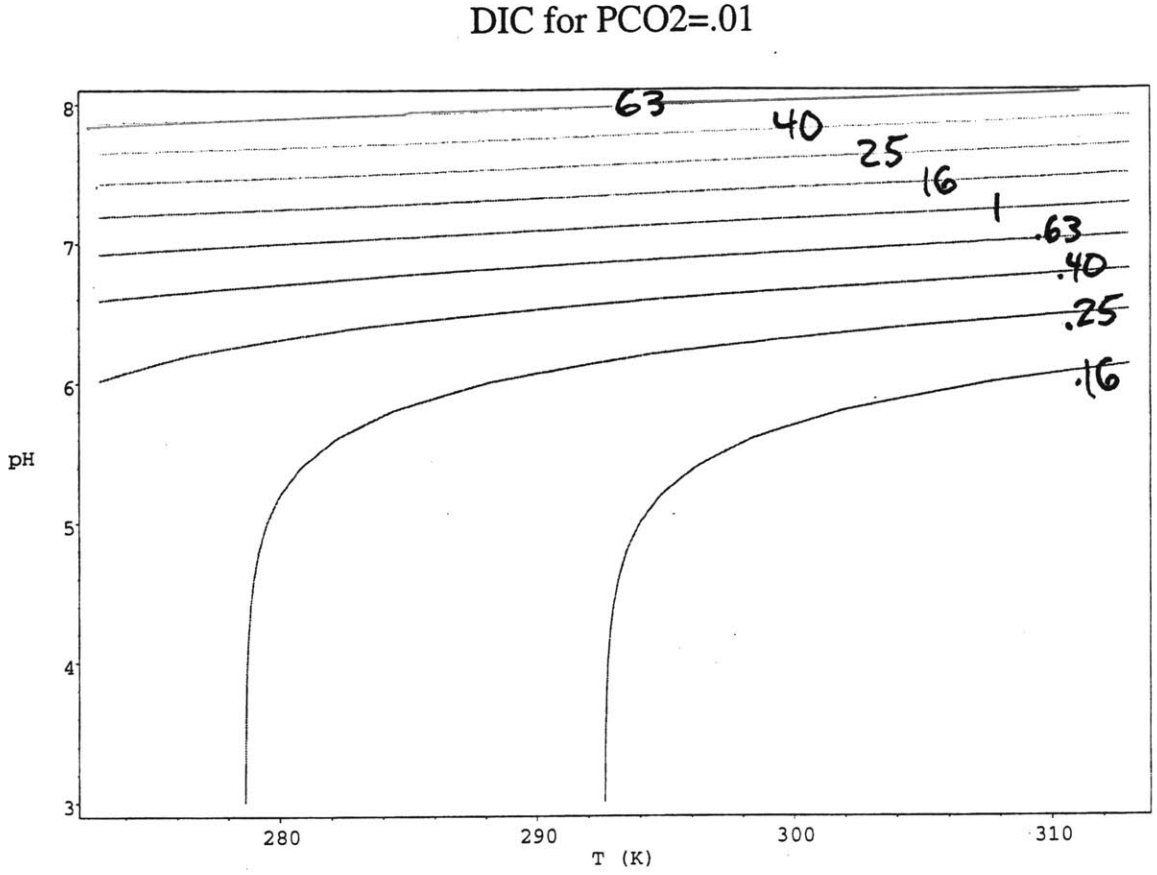

Figure 14. DIC (mol/l) shown in contours, as a function of pH and temperature (K). One can see that for pH below about 5.5, the DIC is not sensitive to changes in pH. For higher pH, DIC is more sensitive to pH changes. Temperature does not have as great an effect.

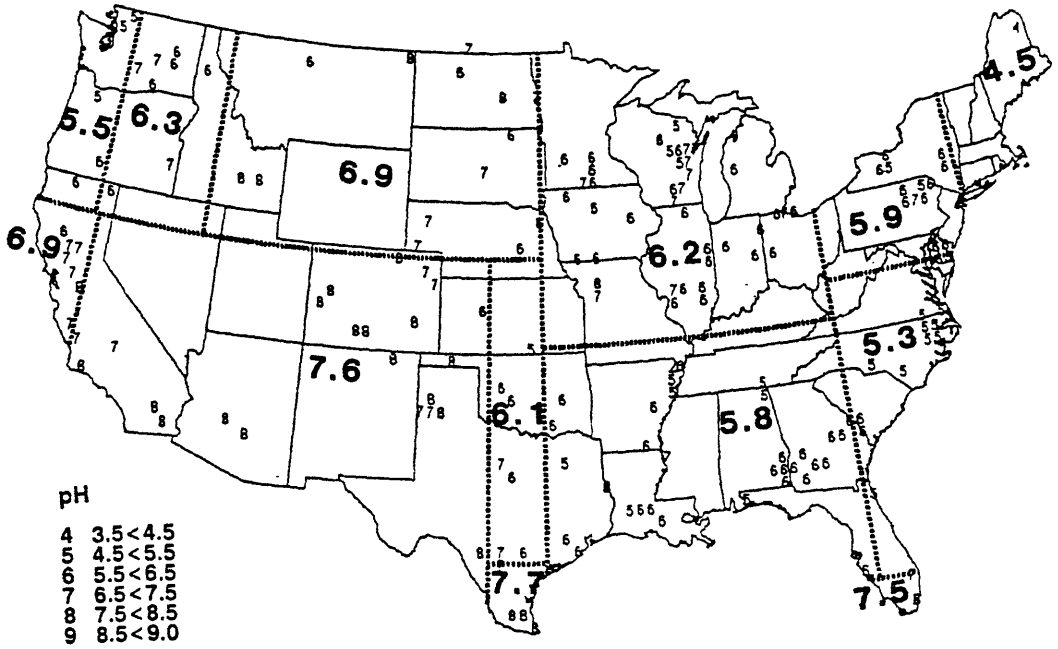

Figure 15. Geographic distribution of pH in U.S. soils. The bold numbers are means for the selected areas, while the small numbers are county average concentrations. (Holmgren 1993)

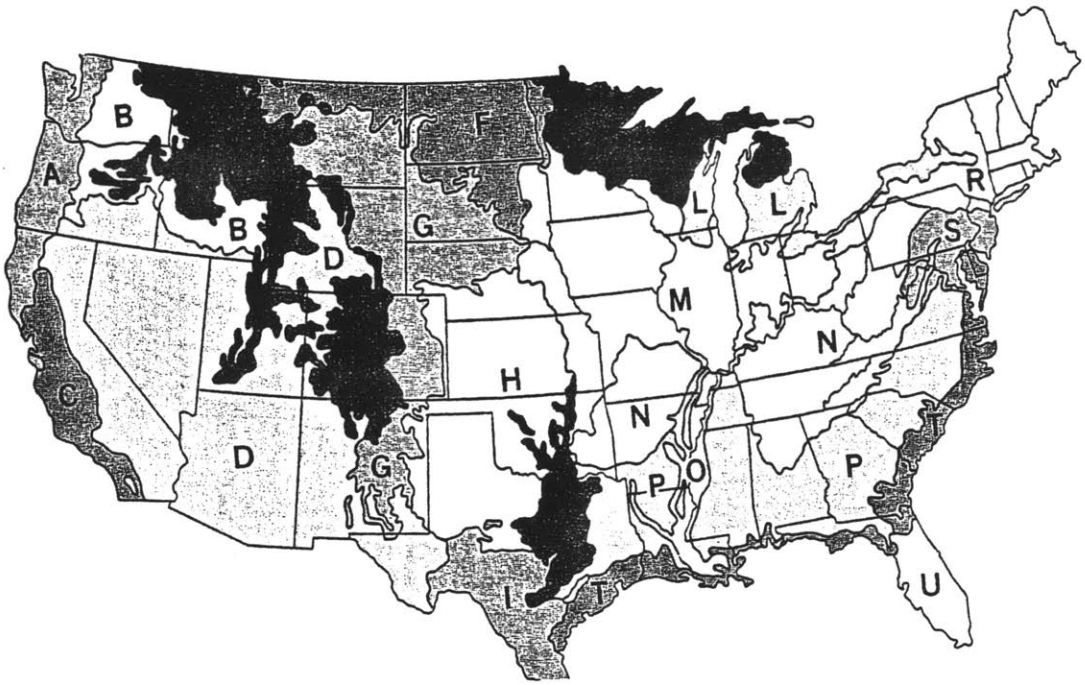

Figure 16. Land resource areas corresponding to **Table 7** (Holmgren 1993)

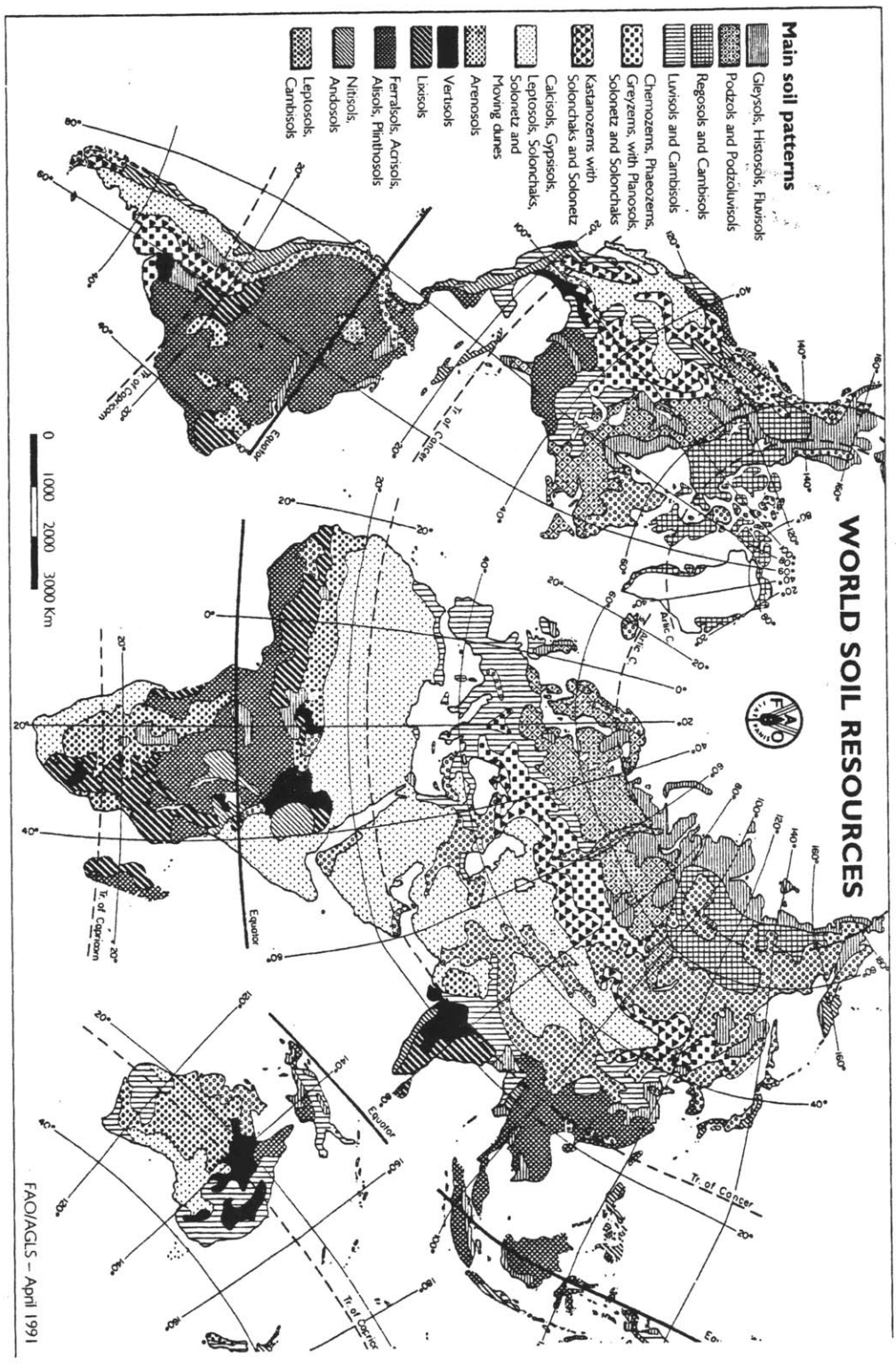

Figure 17. Generalized soil map of the world from Report No. 66, 1991, FAO, printed in Bridges (Bridges 1997)

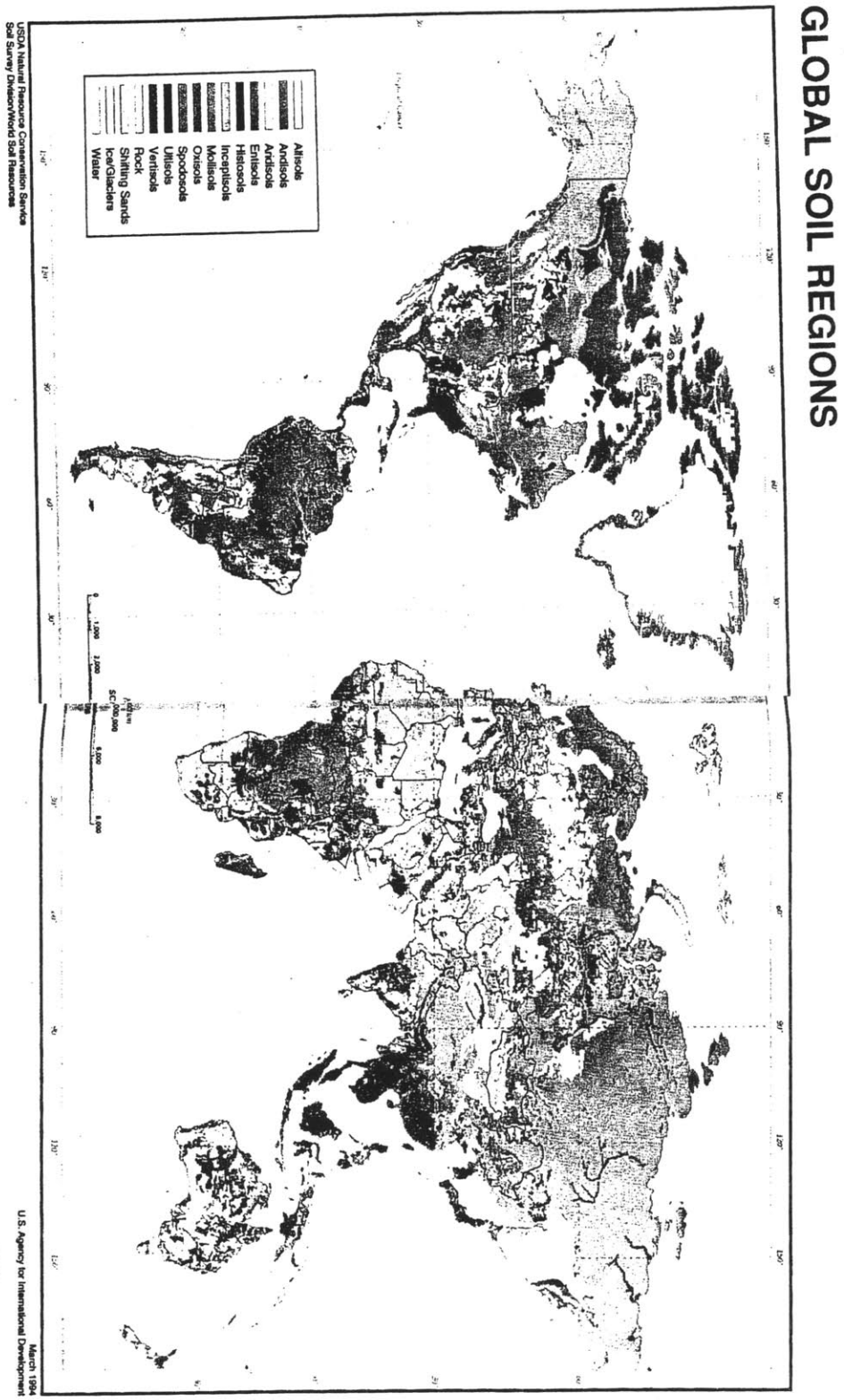

Figure 18. Generalized soil map of the world with U.S. soil classification system (Service 1994)

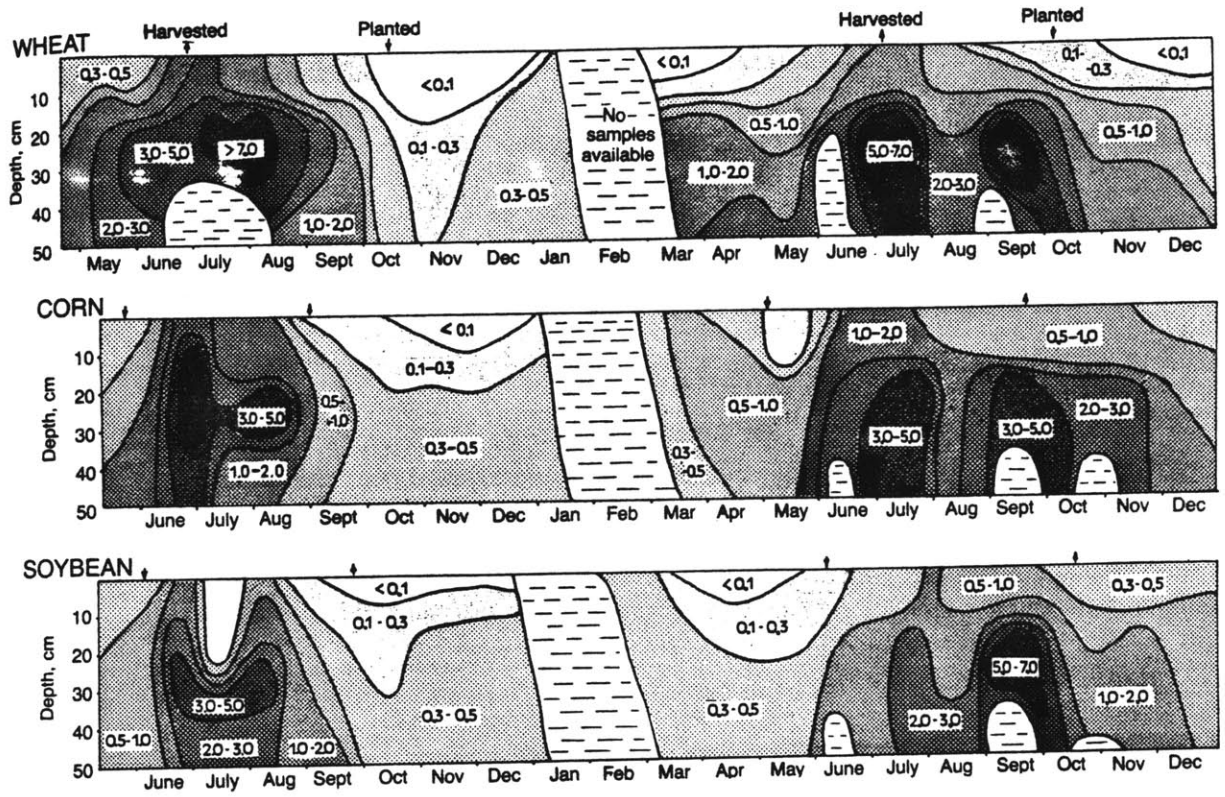

Figure 19. Graphs showing PCO_2 as a function of depth and time for three different crops grown in Mexico (Buyanovsky 1983)

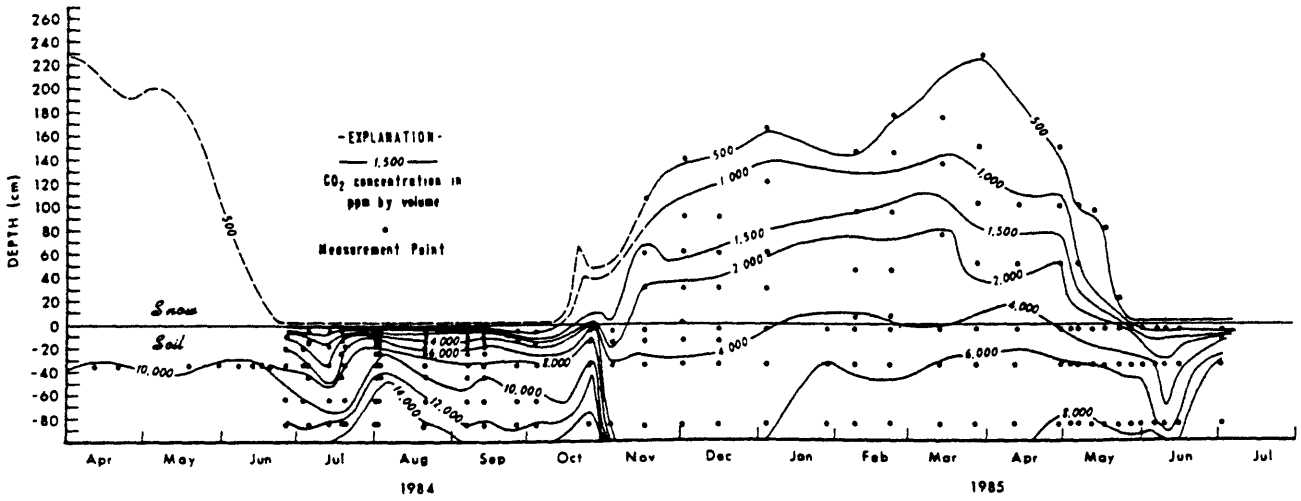

Figure 20. Contours of PCO_2 as a function of depth and time at Brighton, Utah (Solomon 1987)

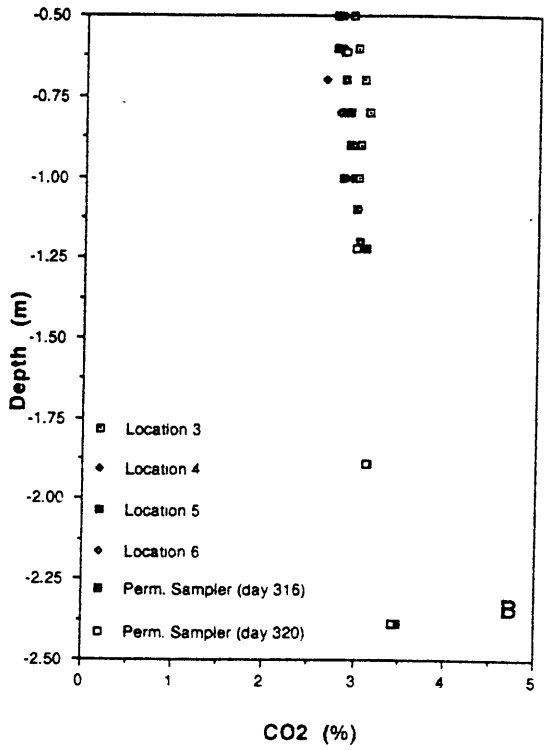

Figure 21. Graph of PCO_2 as a function of depth for a soil in Saskatchewan, Canada (Hendry 1993)

Solve 1-D Fick's law, for the PCO2 at the water table, starting with PCO2 at depth z1

Define C=PCO2 in the soil, q is the the source, assumed constant for all depths
Dfick is the diffusion constant, z=depth, D=depth of water table, and C0=atmospheric PCO2

$$ode := Dfick\left(\frac{\partial^2}{\partial z^2}C(z)\right) = -q$$

$$IC1 := C(0) = C_0$$

$$IC2 := \frac{\partial}{\partial D}C(D) = 0$$

$$solution := C(z) = -\frac{1}{2}\frac{q\,z^2}{Dfick} + \frac{q\,D\,z}{Dfick} + C_0$$

Define F=q/Dfick, solve for F for a given depth z1, atmospheric C0, and C(z1)

$$soln1 := C(z_1) = -\frac{1}{2}\frac{q\,z_1^{\,2}}{Dfick} + \frac{q\,D\,z_1}{Dfick} + C_0$$

$$const := F = \frac{q}{Dfick}$$

$$\left\{q = -2\frac{(C(z_1) - C_0)\,Dfick}{z_1\,(z_1 - 2\,D)},\ F = -2\frac{C(z_1) - C_0}{z_1\,(z_1 - 2\,D)}\right\}$$

Solve for the PCO2 at depth z:

$$soln2 := C(z) = -\frac{2\,D\,z\,C(z_1) - 2\,D\,z\,C_0 - z^2\,C(z_1) + z^2\,C_0 - C_0\,z_1^{\,2} + 2\,C_0\,z_1\,D}{z_1\,(z_1 - 2\,D)}$$

Solve for the PCO2 at the water table by setting z=D:

$$soln3 := C(D) = -\frac{D^2\,C(z_1) - C_0\,D^2 - C_0\,z_1^{\,2} + 2\,C_0\,z_1\,D}{z_1\,(z_1 - 2\,D)}$$

$$C(z) = .003684210527\,z - .00009210526319\,z^2 + .003$$

Figure 22. Derivation for PCO_2 versus depth profile, starting from the assumption of a uniform source of CO_2 throughout the soil profile

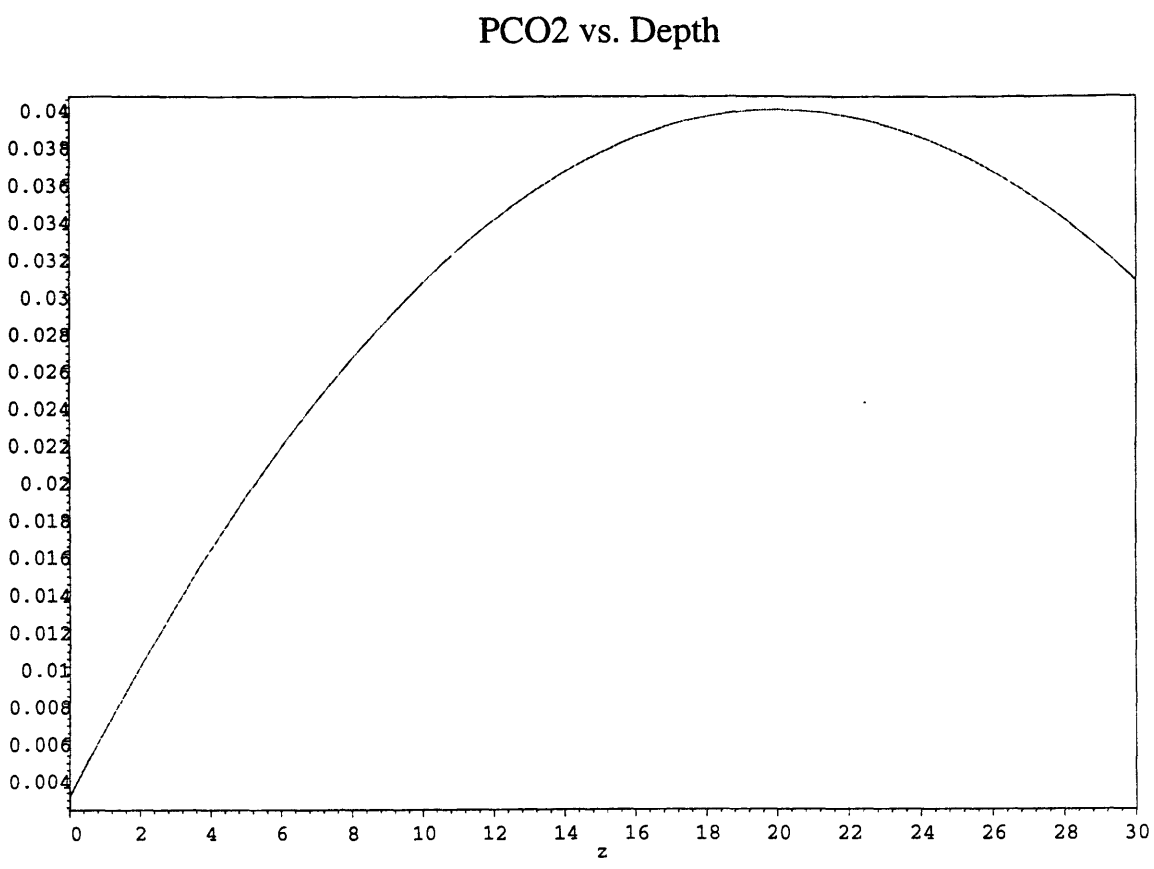

Figure 23. PCO_2 versus depth, as derived in **Figure 22**, for a single PCO_2 measurement of .01 atm, at a depth of 2 m, and atmospheric $PCO_2 = 10^{-3.5}$. The depth of the water table is 30 m.

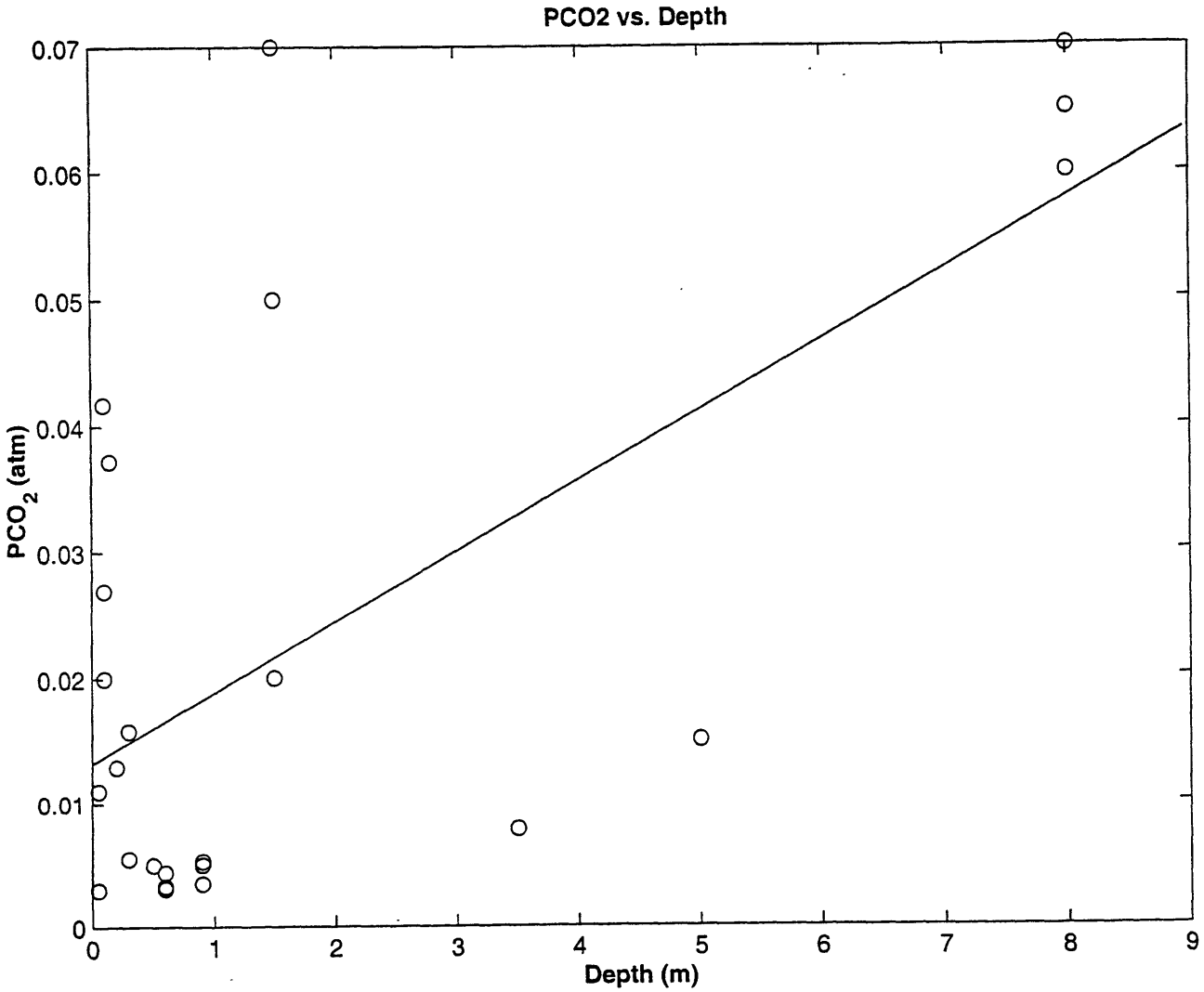

Figure 24. Composite plot for PCO_2 as a function of depth, for data used in this study, with a linear regression line drawn to fit the data

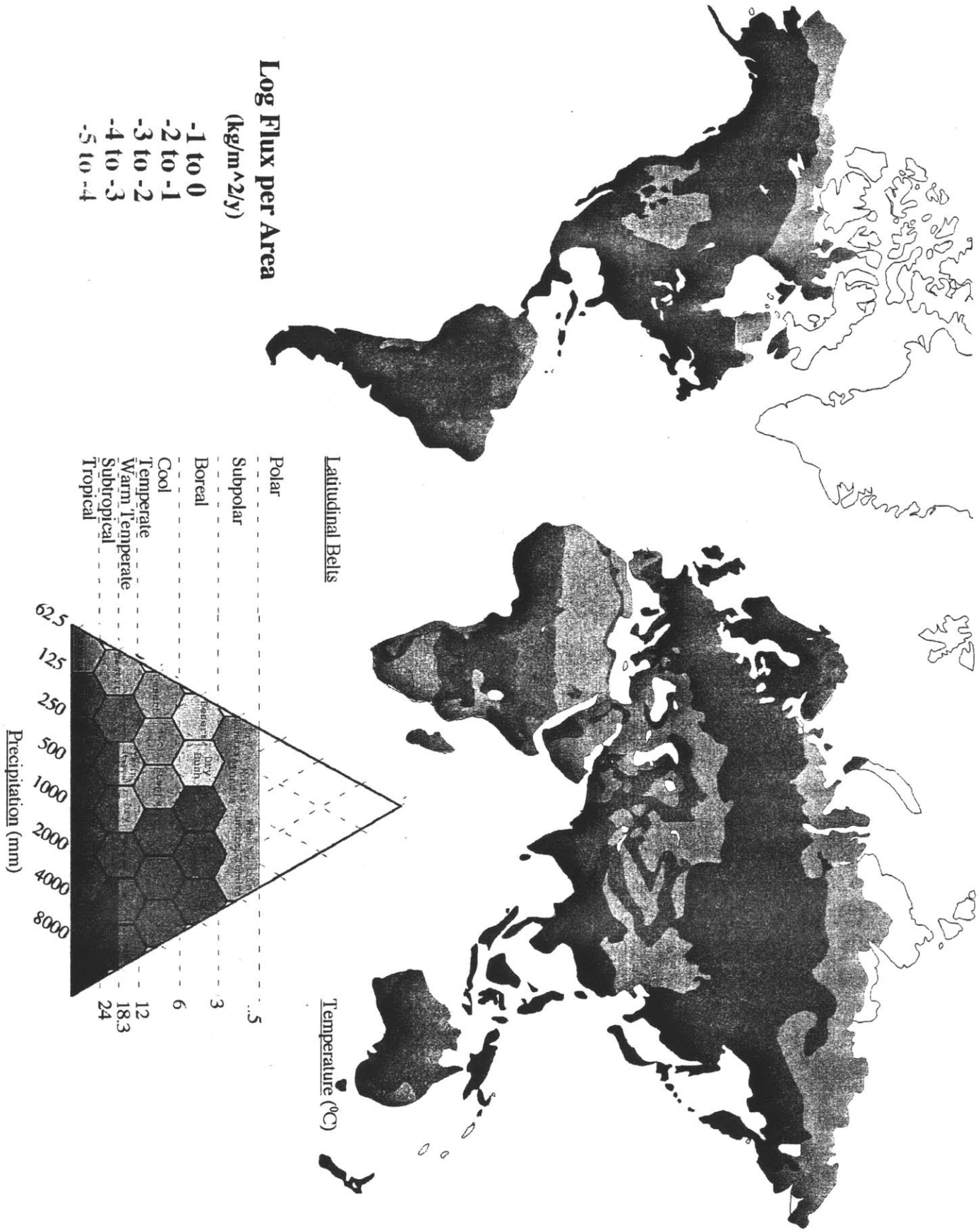

Figure 25. Carbon Flux per Area, calculated for Holdridge life-zones

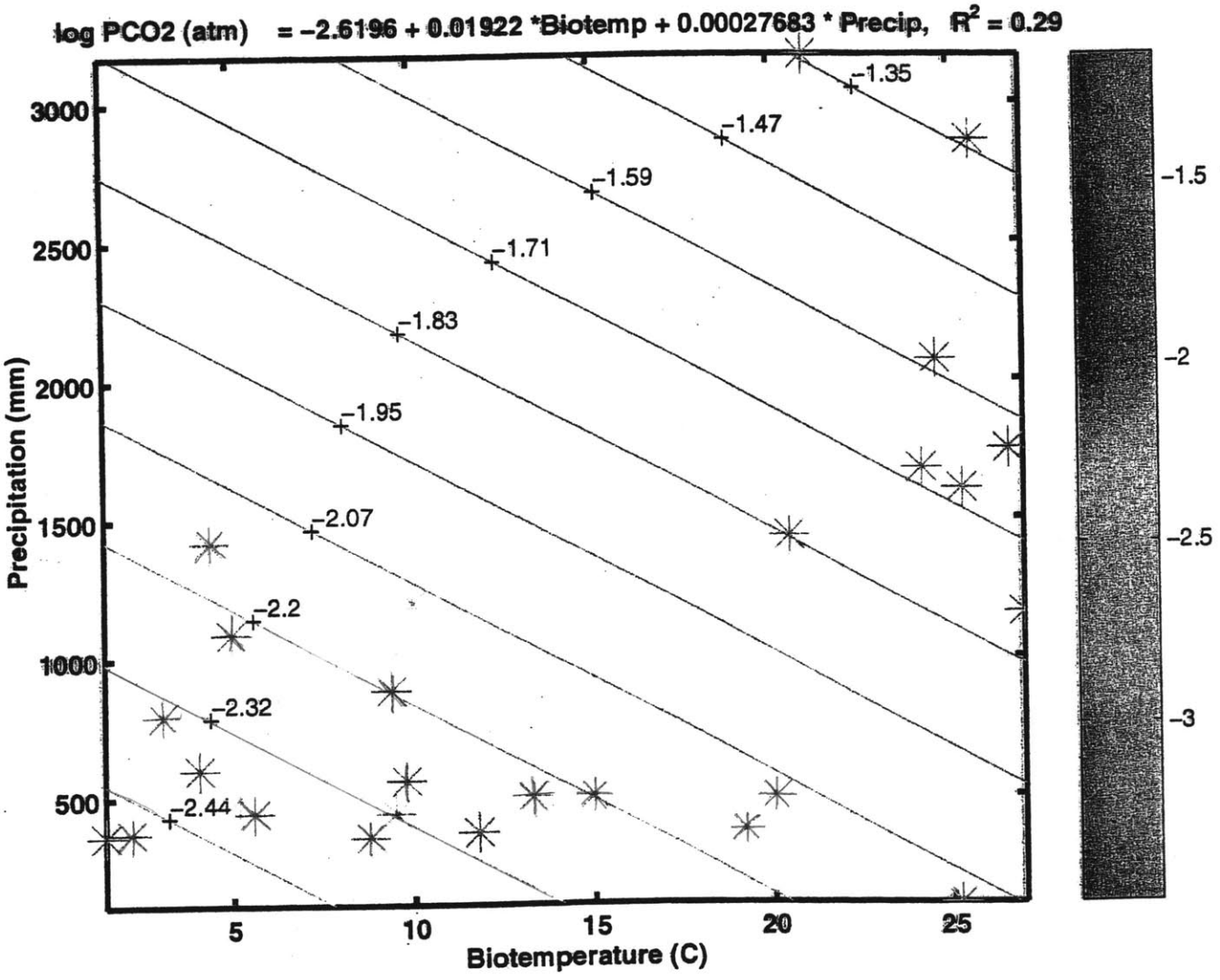

Figure 26. Regression for log(PCO_2) as a function of precipitation and biotemperature. PCO_2 from the regression is plotted as diagonal contour lines, and the measurements used in this study are plotted as stars

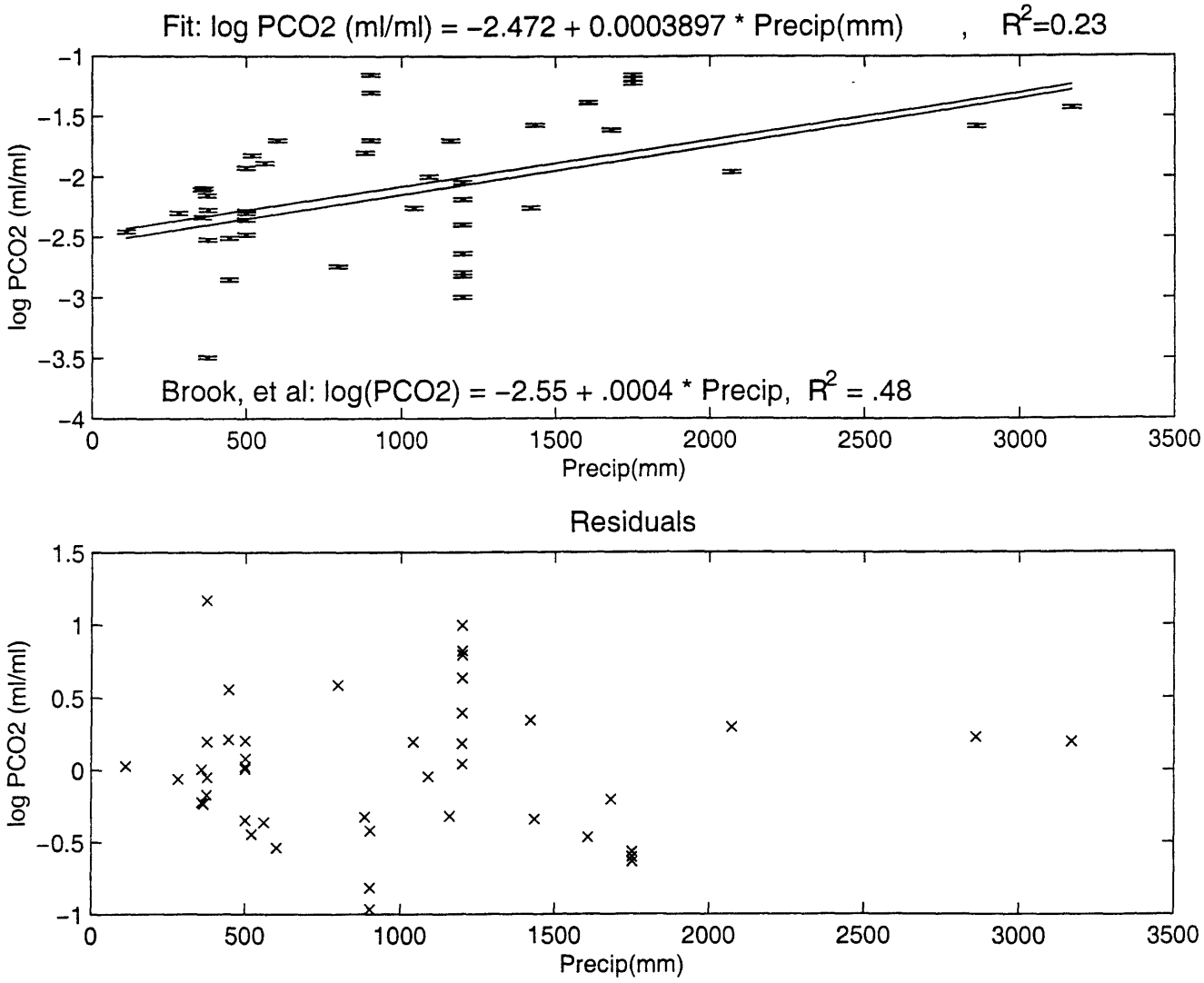

Figure 27. Linear regression between log(PCO_2) and precipitation

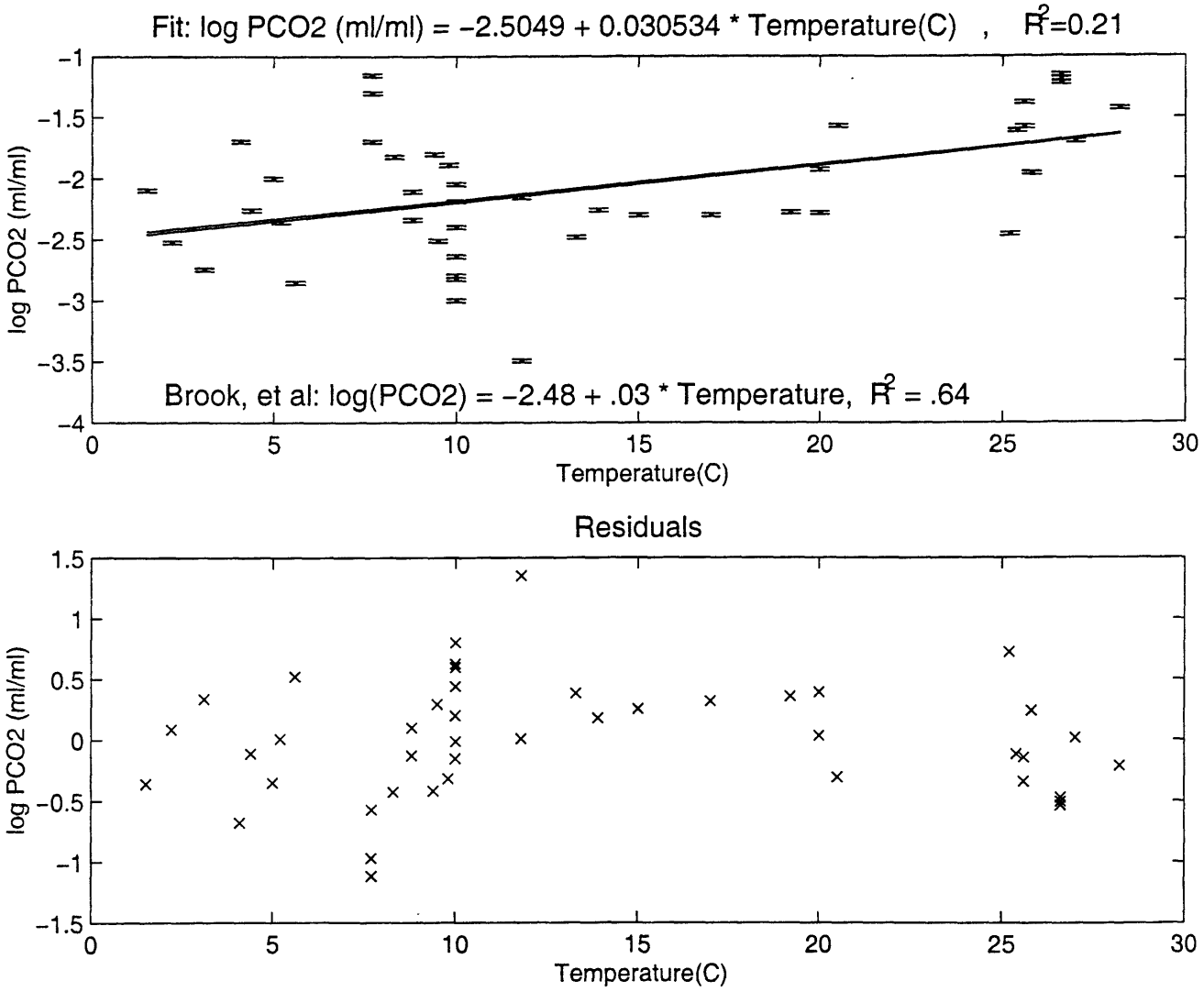

Figure 28. Linear regression between log(PCO_2) and temperature

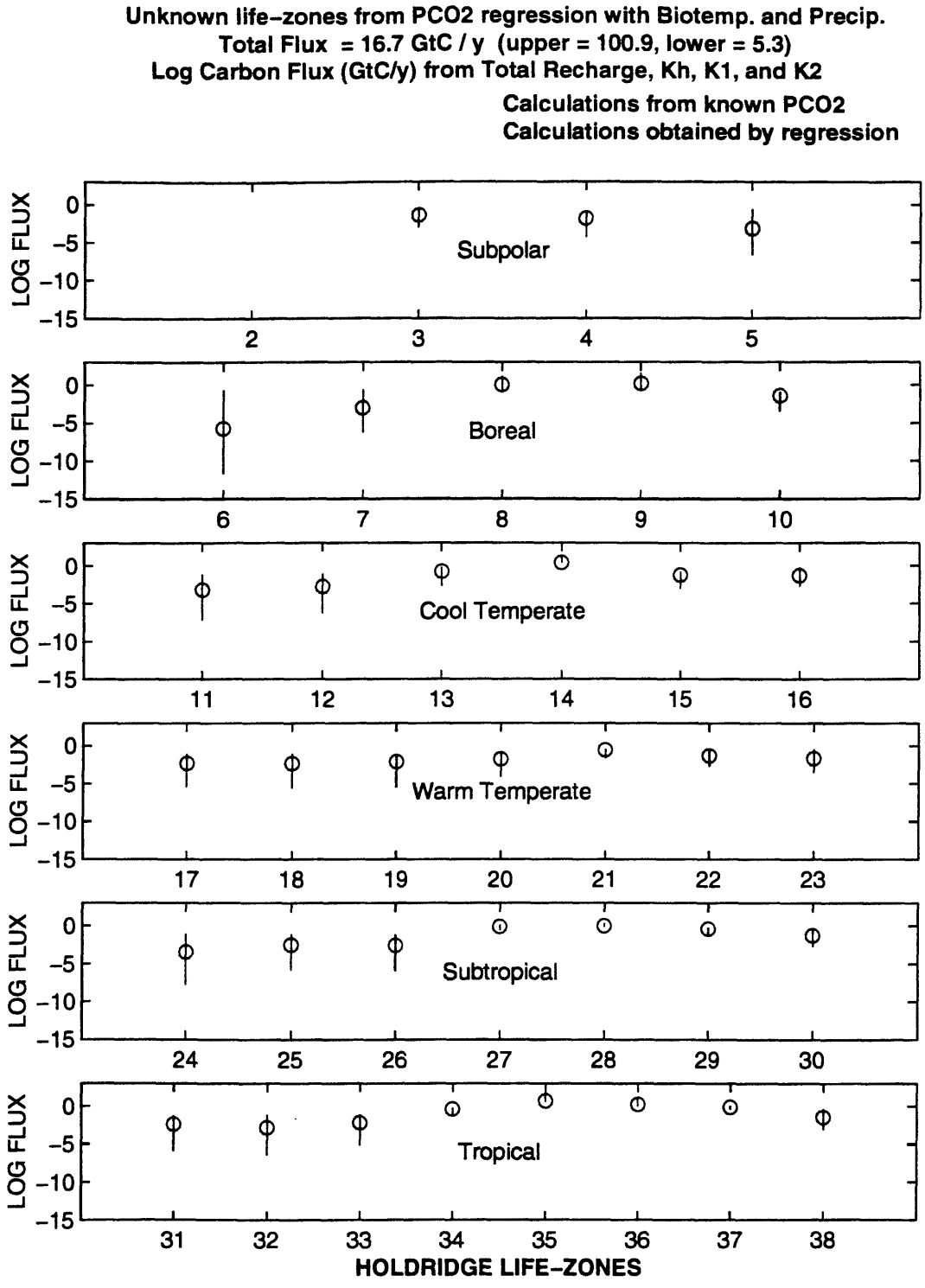

Figure 29. Carbon flux calculated for the Holdridge temperature-regions (excluding the polar region)

Soil order	N	Cd	Zn	Cu	Ni	Pb	CEC	OC	pH
		mg/kg dry soil					cmol/kg	%	
Ultisol	435	0.049 f*	13.8 f	6.2 f	7.4 f	8.0 f	3.5 g	0.78 d	5.60 e
Alfisol	514	0.112 e	31.3 e	10.9 e	12.6 e	9.6 e	9.0 f	0.86 d	6.00 d
Spodosol	37	0.200 d	44.1 d	48.3 b	22.0 cd	10.0 de	9.3 f	1.73 b	4.93 f
Mollisol	936	0.227 cd	54.4 c	19.1 d	22.8 bcd	10.7 d	18.7 c	1.39 c	6.51 c
Vertisol	87	0.239 c	93.1 a	48.5 b	75.9 a	17.1 a	35.6 b	1.32 c	6.72 b
Aridisol	150	0.304 b	70.1 b	25.0 c	24.3 bc	10.6 de	15.2 d	0.63 e	7.26 a
Inceptisol	213	0.230 cd	69.4 b	28.4 c	25.6 b	15.2 b	14.6 d	1.41 c	6.08 d
Entisol	250	0.246 c	65.5 b	21.1 d	21.0 d	10.0 de	11.6 e	0.68 e	7.32 a
Histosol	264	0.622 a	62.6 b	183.2 a	11.3 e	12.5 c	128. a	32.1 a	5.50 e
All	2886	0.178	43.2	18.3	16.9	10.5	14.4	1.41	6.25

* Means within a column followed by the same letter are not significantly different ($P < 0.05$) according to the Waller-Duncan K-ratio T test.

Table 1. Geometric means of selected soil elements and associated soil parameters in U.S. surface soils by taxonomic soil order. (Holmgren 1993)

#	Location	Source	Comments
1	Brazil-Para State	Davidson & Trumbore,1995	forest
2	Brazil-Para State	Davidson & Trumbore,1995	pasture
3	Brazil-Para State	Nepstad, et al,1994	degraded pasture
4	Canada-East central Alberta	Wallick,1981	Glacia drift aquifer, pH from field,alt.=700 m.
5	Canada-East central Alberta	Wallick,1981	Bedrock Aquifer, everything else the same as above
6	Canada-Newfoundland	Brook,et al, 1982	
7	Canada-Rocky Mountains	Brook, et al,1982	
8	Canada-Saskatcewan	Brook, et al,1982	
9	Canada-Saskatoon, Sask.	Keller,1991	measured DIC=.048 +/-.02,clayey till 18 m. thick
10	China-Yunan	Brook, et al,1982	
11	Germany-Frankfurt-Main	Brook, et al,1982	
12	Germany-Mullenbach	Brook, et al,1982	
13	Hot Springs,UT	Hinkle, 1994	May-Aug.
14	Hot Springs,UT	Hinkle, 1994	Nov.-Aug.
15	Jamaica	Brook, et al,1982	
16	Mexico	Buyanovsky and Wagner,1983	upland claypan silt loam soil, Udollic Ochraqualf
17	Namibia-Witvlei	Lovell,et al,1983	160 km E of Windhoek
18	NW Europe	Russell,1973	soil/veg. = arable
19	NW Europe	Russell,1973	soil/veg. = pasture
20	NW Europe	Russell,1973	soil/veg. = sandy arable
21	NW Europe	Russell,1973	soil/veg. = arable loam
22	NW Europe	Russell,1973	soil/veg. = Moorland
23	NW Europe	Russell,1973	soil/veg. = arable
24	NW Europe	Russell,1973	soil/veg. = manured arable
25	Puerto Rico	Brook, et al,1982	
26	Russia-near Moscow	Trainer,et al, 1976	clay loam under mixed forest, July-Dec.
27	Saudi Arabia-Ash Shai'ib	Lovell,et al,1983	
28	Suluwesi	Brook, et al,1982	soil type?
29	Thailand	Jugsujinda,et al,1996	25 acid-sulfate soils, Typic tropoaquept, CO2 lab-measure
30	Thailand-Phangna	Brook, et al,1982	
31	Trinidad	Brook, et al,1982	wet and dry
32	U.S. Los Alamos, NM	Kunkler, 1969	Bandalier tuff, reservoir gas, thin soil
33	U.S. Los Alamos, NM	Kunkler, 1969	Bandalier tuff, reservoir gas, thin soil
34	U.S., west TX	Thorstenson,et al,1983	Oglala aquifer
35	U.S., west TX	Thorstenson,et al,1983	Oglala aquifer
36	U.S.-Brighton, UT	Solomon and Cerling,1987	soil=mixed typic cryochrept,bedrock at 1.5m
37	U.S.-Golden, CO	Hinkle, 1994	sand,silt loam, March-June
38	U.S.-Golden, CO	Hinkle, 1994	March-June
39	U.S.-Johnson Camp,AZ	Lovell,et al,1983	100 km SE of Tucson, alkaline sand, caliche
40	U.S.-near Ithaca, NY	Boynton,et al,1943	silty clay
41	U.S.-near Ithaca, NY	Boynton,et al,1943	sandy loam
42	U.S.-near Ithaca, NY	Boynton,et al,1943	light silty clay loam
43	U.S.-Pullman,WA	Wood,et al,1993	silt loam (loess) 10m thick
44	U.S.-Reston,VA	Brook,et al, 1982	

Table 2. PCO_2 measurements and their locations as plotted in **Figure 10**

#	PCO2 (mL/mL)	pH	T (deg. C)	Depth (m)	Depth (m) water table	P (mm/y)	Rtotal (mm/y)
1	0.07			8	45	1750	
2	0.065			8	45		
3	0.06			8	45		
4	0.007	7.5	11.8	20		373	
5	0.00032	7.5	11.8	20		373	
6	0.0055		4.4			1420	950
7	0.0018		3.1			797	414
8	0.003		2.2	0.05		374	17
9	0.008			8.9			
10	0.0269		20.5	0.1		1434	571
11	0.0129		9.8	0.2		560	10
12	0.0158		9.4	0.3		885	265
13	0.0033		13.3	0.6			
14	0.0044		5.2	0.6			
15	0.011		25.8	0.05		2072	1132
16	0.005	5.3	15	0.5			
17	0.0053			0.9		375	
18	0.009						
19	0.001						
20	0.0016						
21	0.0023						
22	0.0065						
23	0.0015						
24	0.004						
25	0.0245		25.4			1680	286
26	0.02			1.5			
27	0.0035			0.9			
28	0.0263		25.6			2862	1557
29	0.02	4		0.1			
30	0.0372		28.2	0.15		3168	1422
31	0.0417		25.6	0.1		1606	317
32	0.0046			86	300		
33	0.0078			3.5	300		
34	0.0118			21.4	77		
35	0.0052			44.5	51		
36	0.01		5	10	6	1090	
37	0.0031		9.5	0.6			
38	0.0014		5.6	0			
39	0.005			0.9		280	
40	0.07			1.5	1.5	902	
41	0.05			1.5	1.5	902	
42	0.02			1.5	1.5	902	
43	0.015		8.3	5	6	520	80
44	0.0055		13.9	0.3		1041	318

#	PCO2 (mL/mL)	pH	T (deg. C)	Depth (m)	Depth (m) water table	P (mm/y)	Rg	Rtotal	Holdridge Life-zone
1	0.07	5.8	26.6	8	45	1750	200	1200	28
2	0.065	5.8	26.6	8	45	1750	200	1200	28
3	0.06	5.8	26.6	8	45	1750	200	1200	28
4	0.007	7.5	11.8	20		373	1	75	13
5	0.00032	7.5	11.8	20		373	1	75	13
6	0.0055	4.93	4.4			1420	200	1000	10
7	0.0018	7.8	3.1			797	414	1000	9
8	0.003	6.5	2.2	0.05		374	17	50	4
9	0.008	6.5	1.5	8.9		363	17	50	4
10	0.0269	5.6	20.5	0.1		1434	571	800	27
11	0.0129	6.1	9.8	0.2		560	10	400	14
12	0.0158	6.1	9.4	0.3		885	265	400	14
13	0.0033	6.25	13.3	0.6		500	5	25	20
14	0.0044	6.25	5.2	0.6		500	5	25	20
15	0.011	5.2	25.8	0.05		2072	400	1132	29
16	0.005	5.3	15	0.5		500	1	10	20
17	0.0053	7.3	19.2	0.9		375	1	5	24
18	0.009	6	10			1200	100	500	15
19	0.001	6	10			1200	100	500	15
20	0.0016	6	10			1200	100	500	15
21	0.0023	6	10			1200	100	500	15
22	0.0065	6	10			1200	100	500	15
23	0.0015	6	10			1200	100	500	15
24	0.004	6	10			1200	100	500	15
25	0.0245	6.25	25.4			1680	286	1500	28
26	0.02	3.5	4.1	1.5		601	75	175	9
27	0.0035	7.7	25.2	0.9		110	1	5	24
28	0.0263	5	25.6			2862	300	1500	29
29	0.02	4	27	0.1		1160	200	1000	21
30	0.0372	5.2	28.2	0.15		3168	300	1422	22
31	0.0417	5.2	25.6	0.1		1606	317	1500	28
32	0.0046	7.6	8.8	86	300	357	1	5	13
33	0.0078	7.6	8.8	3.5	300	357	1	5	13
34	0.0118	6.7	20	21.4	77	500	1	7	19
35	0.0052	6.7	20	44.5	51	500	1	7	19
36	0.01	6.8	5	10	6	1090	1	300	10
37	0.0031	7.8	9.5	0.6		445	1	7	13
38	0.0014	7.8	5.6	0		445	1	7	13
39	0.005	7.6	17	0.9		280	1	1	19
40	0.07	5.3	7.7	1.5	1.5	902	150	600	14
41	0.05	5.3	7.7	1.5	1.5	902	150	600	14
42	0.02	5.3	7.7	1.5	1.5	902	150	600	14
43	0.015	6	8.3	5	6	520	80	100	14
44	0.0055	5.8	13.9	0.3		1041	100	318	27

Table 3. Complete set of parameters used for the calculations in this study

T (K)	pH	p(PCO2)	p(Kh)	pK1	pK2	pKw	KhK1(PCO2)/[H+]	2KhK1K2(PCO2)/[H+]^2	Kw/[H+]
273	3	3.5	1.105767983	6.580583359	10.63092031	14	6.51101E-09	3.0462E-16	1E-11
273	5	3.5	1.105767983	6.580583359	10.63092031	14	6.51101E-07	3.0462E-12	0.000000001
273	7	3.5	1.105767983	6.580583359	10.63092031	14	6.51101E-05	3.0462E-08	0.0000001
273	8	3.5	1.105767983	6.580583359	10.63092031	14	0.000651101	3.0462E-06	0.000001
273	3	2.5	1.105767983	6.580583359	10.63092031	14	6.51101E-08	3.0462E-15	1E-11
273	5	2.5	1.105767983	6.580583359	10.63092031	14	6.51101E-06	3.0462E-11	0.000000001
273	7	2.5	1.105767983	6.580583359	10.63092031	14	0.000651101	3.0462E-07	0.0000001
273	8	2.5	1.105767983	6.580583359	10.63092031	14	0.006511014	3.0462E-05	0.000001
273	3	1.5	1.105767983	6.580583359	10.63092031	14	6.51101E-07	3.0462E-14	1E-11
273	5	1.5	1.105767983	6.580583359	10.63092031	14	6.51101E-05	3.0462E-10	0.000000001
273	7	1.5	1.105767983	6.580583359	10.63092031	14	0.006511014	3.0462E-06	0.0000001
273	8	1.5	1.105767983	6.580583359	10.63092031	14	0.065110144	0.00030462	0.000001
283	3	3.5	1.267143543	6.464804341	10.48976845	14	5.86209E-09	3.79589E-16	1E-11
283	5	3.5	1.267143543	6.464804341	10.48976845	14	5.86209E-07	3.79589E-12	0.000000001
283	7	3.5	1.267143543	6.464804341	10.48976845	14	5.86209E-05	3.79589E-08	0.0000001
283	8	3.5	1.267143543	6.464804341	10.48976845	14	0.000586209	3.79589E-06	0.000001
283	3	2.5	1.267143543	6.464804341	10.48976845	14	5.86209E-08	3.79589E-15	1E-11
283	5	2.5	1.267143543	6.464804341	10.48976845	14	5.86209E-06	3.79589E-11	0.000000001
283	7	2.5	1.267143543	6.464804341	10.48976845	14	0.000586209	3.79589E-07	0.0000001
283	8	2.5	1.267143543	6.464804341	10.48976845	14	0.005862085	3.79589E-05	0.000001
283	3	1.5	1.267143543	6.464804341	10.48976845	14	5.86209E-07	3.79589E-14	1E-11
283	5	1.5	1.267143543	6.464804341	10.48976845	14	5.86209E-05	3.79589E-10	0.000000001
283	7	1.5	1.267143543	6.464804341	10.48976845	14	0.005862085	3.79589E-06	0.0000001
283	8	1.5	1.267143543	6.464804341	10.48976845	14	0.058620851	0.000379589	0.000001
293	3	3.5	1.404960842	6.382874675	10.3770617	14	5.15424E-09	4.32646E-16	1E-11
293	5	3.5	1.404960842	6.382874675	10.3770617	14	5.15424E-07	4.32646E-12	0.000000001
293	7	3.5	1.404960842	6.382874675	10.3770617	14	5.15424E-05	4.32646E-08	0.0000001
293	8	3.5	1.404960842	6.382874675	10.3770617	14	0.000515424	4.32646E-06	0.000001
293	3	2.5	1.404960842	6.382874675	10.3770617	14	5.15424E-08	4.32646E-15	1E-11
293	5	2.5	1.404960842	6.382874675	10.3770617	14	5.15424E-06	4.32646E-11	0.000000001
293	7	2.5	1.404960842	6.382874675	10.3770617	14	0.000515424	4.32646E-07	0.0000001
293	8	2.5	1.404960842	6.382874675	10.3770617	14	0.005154238	4.32646E-05	0.000001
293	3	1.5	1.404960842	6.382874675	10.3770617	14	5.15424E-07	4.32646E-14	1E-11
293	5	1.5	1.404960842	6.382874675	10.3770617	14	5.15424E-05	4.32646E-10	0.000000001
293	7	1.5	1.404960842	6.382874675	10.3770617	14	0.005154238	4.32646E-06	0.0000001
293	8	1.5	1.404960842	6.382874675	10.3770617	14	0.051542382	0.000432646	0.000001
303	3	3.5	1.522785192	6.328772304	10.28902954	14	4.45085E-09	4.57555E-16	1E-11
303	5	3.5	1.522785192	6.328772304	10.28902954	14	4.45085E-07	4.57555E-12	0.000000001
303	7	3.5	1.522785192	6.328772304	10.28902954	14	4.45085E-05	4.57555E-08	0.0000001
303	8	3.5	1.522785192	6.328772304	10.28902954	14	0.000445085	4.57555E-06	0.000001
303	3	2.5	1.522785192	6.328772304	10.28902954	14	4.45085E-08	4.57555E-15	1E-11
303	5	2.5	1.522785192	6.328772304	10.28902954	14	4.45085E-06	4.57555E-11	0.000000001

Table 4. Test to show that $K_1K_2/[H^+]^2$ and $K_w/[H^+]$ are negligible for realistic limits of T, pH, and PCO_2

303	7	2.5	1.522785192	6.328772304	10.28902954	14	0.000445085	4.57555E-07	0.0000001
303	8	2.5	1.522785192	6.328772304	10.28902954	14	0.004450845	4.57555E-05	0.000001
303	3	1.5	1.522785192	6.328772304	10.28902954	14	4.45085E-07	4.57555E-14	1E-11
303	5	1.5	1.522785192	6.328772304	10.28902954	14	4.45085E-05	4.57555E-10	0.000000001
303	7	1.5	1.522785192	6.328772304	10.28902954	14	0.004450845	4.57555E-06	0.0000001
303	8	1.5	1.522785192	6.328772304	10.28902954	14	0.044508453	0.000457555	0.000001
313	3	3.5	1.623531936	6.297706289	10.22254157	14	3.79107E-09	4.54203E-16	1E-11
313	5	3.5	1.623531936	6.297706289	10.22254157	14	3.79107E-07	4.54203E-12	0.000000001
313	7	3.5	1.623531936	6.297706289	10.22254157	14	3.79107E-05	4.54203E-08	0.0000001
313	8	3.5	1.623531936	6.297706289	10.22254157	14	0.000379107	4.54203E-06	0.000001
313	3	2.5	1.623531936	6.297706289	10.22254157	14	3.79107E-08	4.54203E-15	1E-11
313	5	2.5	1.623531936	6.297706289	10.22254157	14	3.79107E-06	4.54203E-11	0.000000001
313	7	2.5	1.623531936	6.297706289	10.22254157	14	0.000379107	4.54203E-07	0.0000001
313	8	2.5	1.623531936	6.297706289	10.22254157	14	0.00379107	4.54203E-05	0.000001
313	3	1.5	1.623531936	6.297706289	10.22254157	14	3.79107E-07	4.54203E-14	1E-11
313	5	1.5	1.623531936	6.297706289	10.22254157	14	3.79107E-05	4.54203E-10	0.000000001
313	7	1.5	1.623531936	6.297706289	10.22254157	14	0.00379107	4.54203E-06	0.0000001
313	8	1.5	1.623531936	6.297706289	10.22254157	14	0.037910697	0.000454203	0.000001
"p(variable)"=-log(variable)									

Carbonate groundwater, Troutcreek Ontario (Reardon, et a			Mean Annua	Calculated	Calculated
pH	Alk (eq/l)	PCO2 (atm	Temp (C)	DIC (mol/l)	Alk(mol/l)
7.6	0.0038	0.005	4		0.003951
"Bedrock aquifer," Saskatoon, Sask (Keller,1991)					
7.2	0.05	0.01	2	0.003928	

Table 6. Comparisons between measured and calculated DIC and alkalinity

#	Location	Source	Comments
	Not used in calculations:		
45	U.S.-Gascoyne, ND (sw ND)	Haas, et al,1983	water table above lignite, total P=.91 atm.
46	U.S.-Gascoyne, ND (sw ND)	Haas, et al,1983	in lignite layer,PCO2 very high
47	U.S.-Gascoyne, ND (sw ND)	Thorstenson,et al,1983	lignite rich
48	U.S.-Gascoyne, ND (sw ND)	Thorstenson,et al,1983	lignite just above g/w
49	U.S.-Gascoyne, ND (sw ND)	Thorstenson,et al,1983	lignite rich
50	Brazil-Para State	Nepstad, et al,1994	karst soils
51	Canada-Bruce Peninsula	Brook, et al,1982	Brook values for Rtot=P-ET
52	Canada-Trout Creek,Ont.	Reardon, et al,1982	5 km SE of Delhi, Ontario
53	U.S.-Alaska	Brook, et al,1982	T=-3.6
54	U.S.-Sinking Cove,TN	Brook, et al,1982	
55	U.S.-Mammoth Cave,KY	Brook, et al,1982	
56	U.S.,South FL	Brook, et al,1982	
57	Canada-Mohanni	Brook, et al,1982	T=-4.5
58	U.K.-Mendip Hills	Atkinson,1977	limestone. "percolation" water
59	?	Gerstenhauer in Atkinson,1976	soil/veg. = sandy loam
60	?	Nicholson in Atkinson,1976	soil/veg. = "brown earth"
61	?	Sheikh,1969,in Atkinson,1976	soil/veg. = "valley bog"

Table 7. PCO_2 measurements not used in calculations

Land resource region	N	Cd	Zn	Cu	Ni	Pb	CEC	OC	pH
		mg/kg dry soil					cmol/kg	%	
Mineral soils									
A Northwestern specialty	58	0.247 cd*	64.9 bc	34.3 b	36.6 b	9.2 efg	19.2 a	2.46 a	5.45 jk
B Northwestern wheat	170	0.202 ef	61.1 cd	23.2 cd	24.0 cd	8.1 ghi	14.5 bc	0.79 ghi	6.68 d
C California subtropical	206	0.254 bcd	90.4 a	43.4 a	64.4 a	10.6 cd	19.7 a	0.91 f	7.07 c
D Western range and irrigated	120	0.291 bc	73.8 b	26.8 c	25.2 cd	9.6 def	13.4 bcd	0.53 l	7.55 b
E Rocky Mountain	40	0.302 b	105. a	19.1 ef	12.7 g	13.2 b	11.3 de	0.64 jk	7.83 a
F Northern Great Plains	73	0.369 a	68.3 bc	20.2 de	27.0 cd	10.0 de	20.8 a	1.76 b	6.81 d
G Western Great Plains	125	0.271 bcd	54.3 d	16.3 fg	17.2 ef	11.8 bc	16.0 b	0.89 fg	7.55 b
H Central Great Plains	181	0.172 fg	36.1 ef	12.6 i	15.3 f	9.2 efg	12.6 cd	0.83 fgh	6.70 d
I Southwest Plateau	180	0.143 g	38.1 ef	10.0 j	12.5 g	7.0 j	11.3 de	0.60 kl	7.46 b
J Southwest Prairie	75	0.046 j	8.8 j	4.9 m	6.5 j	5.0 k	3.7 h	0.42 m	5.71 hi
K Northern lake states	43	0.177 f	40.7 e	15.4 gh	12.3 gh	7.2 ij	7.6 f	1.18 e	5.54 ij
L Lake states	145	0.232 de	60.6 cd	18.2 efg	19.1 e	13.0 b	14.7 bc	1.74 bc	6.31 e
M Central feed grains	407	0.249 cd	61.6 cd	19.7 de	24.1 cd	15.2 a	22.1 a	1.93 b	6.00 f
N East & central farming	21	0.085 h	25.6 g	8.0 k	10.5 h	8.5 fgh	5.3 g	0.68 jk	5.07 l
O Mississippi Delta	116	0.203 ef	61.7 cd	21.1 de	23.7 d	16.4 a	20.1 a	1.30 de	5.95 fg
P South Atlantic & Gulf slope	319	0.047 j	13.5 i	6.3 l	8.2 i	7.7 hij	3.9 h	0.74 hij	5.85 fgh
R Northeastern forage	87	0.176 f	70.8 bc	34.0 b	28.1 c	16.0 a	9.6 e	1.49 d	5.26 kl
S Northern Atlantic slope	118	0.094 h	34.5 f	13.5 hi	11.3 gh	13.0 b	4.3 h	0.71 ij	5.77 gh
T Atlantic and Gulf coast	196	0.065 i	17.1 h	7.6 k	7.8 i	10.0 de	7.6 f	1.13 e	5.30 kl
U Florida subtropical	30	0.375 a	19.9 h	31.9 b	8.0 i	10.1 de	6.8 f	1.51 cd	6.29 e
All Mineral soils	2710	0.156	41.4	15.6	17.4	10.4	11.4	1.02	6.34
Histosols									
K Northern lake states	58	0.742 a	48.5 c	59.6 c	10.3 b	12.2 c	104 c	28.9 d	5.72 a
L Lake states	110	0.693 a	61.9 b	84.7 b	11.6 b	15.0 b	133 b	32.5 c	5.48 b
R Northeastern forage	37	0.691 a	60.7 b	149.0 a	15.6 a	21.7 a	157 a	35.2 b	5.19 c
U Florida subtropical	59	0.357 b	97.8 a	94.3 b	8.0 c	6.0 d	138 ab	39.2 a	5.60 ab
All Histosols	264	0.606	64.8	86.9	10.9	12.3	130	33.4	5.52

* Means within a column, within histosols or mineral soils, followed by the same letter are not significantly different ($P < 0.05$) according to the Waller-Duncan *K*-ratio *T*-test.

Table 8. Land resource regions of the U.S., the pH is on the far right (Holmgren 1993)

		Texture index	pH($CaCl_2$)	El. cond. 10^{-4} S/cm	$CaCO_3$ equiv. %	CEC me/100 g	Org. C %	N total %	P (extractable) mg/l	K (extractable) mg/l	Ca (extractable) mg/l	Mg (extractable) mg/l	Na mg/l
Acrisols	$\bar{x}$	42	5.19	1.2	0.0	19.4	1.1	0.122	15.0	156	1208	238	14
(n = 73)	s	16	0.49	0.9	0.0	11.1	0.7	0.059	14.7	97	653	174	15
Andosols	$\bar{x}$	33	5.26	1.9	0.4	35.5	2.6	0.297	16.7	388	1581	111	14
(n = 8)	s	14	0.63	0.9	0.7	13.0	1.9	0.157	6.8	226	803	94	13
Arenosols	$\bar{x}$	19	5.13	1.6	0.2	13.7	1.1	0.107	82.2	163	793	83	13
(n = 22)	s	8	0.83	1.0	0.2	8.1	0.6	0.053	58.8	89	682	86	11
Cambisols	$\bar{x}$	40	6.41	1.8	2.1	22.2	1.8	0.159	29.5	179	2549	271	46
(n = 246)	s	13	1.27	1.0	5.7	12.3	2.2	0.136	29.4	104	1688	186	77
Chernozems	$\bar{x}$	47	7.20	2.3	5.6	28.1	1.6	0.183	30.4	174	5350	289	16
(n = 48)	s	7	0.70	0.7	5.1	4.3	0.4	0.044	15.4	49	1609	171	18
Ferralsols	$\bar{x}$	32	5.26	0.9	0.0	14.2	1.3	0.116	12.6	112	813	136	9
(n = 127)	s	13	0.74	0.5	0.1	5.3	0.5	0.049	18.2	72	632	89	7
Fluvisols	$\bar{x}$	51	7.44	5.2	7.6	33.4	1.1	0.123	18.1	475	5859	904	397
(n = 470)	s	16	0.68	6.8	9.6	13.9	0.5	0.073	21.2	327	2539	613	543
Gleysols	$\bar{x}$	36	5.62	2.1	0.8	21.3	1.7	0.179	47.2	206	1600	269	17
(n = 31)	s	14	1.00	1.1	2.3	12.7	1.2	0.116	40.8	131	1504	276	17
Halosols	$\bar{x}$	50	7.78	12.3	21.0	23.7	0.8	0.097	10.7	265	6017	780	713
(n = 60)	s	9	0.29	11.8	11.2	6.0	0.3	0.036	13.1	142	1964	336	767
Histosols	$\bar{x}$	—	4.54	2.2	0.0	82.0	20.3	0.968	44.2	151	2079	320	22
(n = 7)	s	—	0.51	0.7	0.0	15.3	9.6	0.412	13.7	54	1068	243	16
Kastanozems	$\bar{x}$	52	7.43	3.2	11.2	34.7	0.9	0.105	12.3	530	7053	674	135
(n = 64)	s	15	0.50	3.6	16.5	15.9	0.3	0.032	12.4	267	3535	393	214
Lithosols	$\bar{x}$	40	7.25	1.3	10.4	26.6	0.8	0.088	8.2	356	5786	305	8
(n = 23)	s	18	0.64	0.4	11.6	12.7	0.4	0.046	4.4	158	3231	155	3
Luvisols	$\bar{x}$	43	6.79	1.9	7.7	24.1	1.0	0.105	24.0	244	4127	404	53
(n = 217)	s	14	0.98	1.3	12.6	12.4	0.5	0.047	29.4	186	2814	382	115
Nitosols	$\bar{x}$	28	5.60	0.9	0.1	13.9	1.1	0.104	14.9	152	1008	187	5
(n = 106)	s	9	0.85	0.6	0.1	6.8	0.5	0.054	17.6	151	687	168	6
Phaeozems	$\bar{x}$	44	6.08	1.8	1.3	29.1	1.9	0.198	26.4	581	3280	355	34
(n = 307)	s	9	0.88	1.6	3.4	8.1	0.7	0.067	21.4	324	1893	178	112
Planosols	$\bar{x}$	52	6.32	3.3	0.6	37.3	2.2	0.210	24.6	545	4220	625	74
(n = 117)	s	14	1.07	2.2	1.0	8.6	0.8	0.087	12.2	277	2107	343	36
Podzols	$\bar{x}$	23	5.23	1.9	0.0	24.0	3.1	0.221	80.3	182	1460	87	14
(n = 11)	s	8	0.46	0.8	0.0	7.1	1.3	0.079	40.2	91	1619	34	16
Regosols	$\bar{x}$	42	6.62	2.6	5.0	21.8	1.1	0.114	33.8	348	4037	361	151
(n = 42)	s	18	0.97	2.9	10.5	11.9	0.5	0.047	31.2	283	3524	363	484
Rendzinas	$\bar{x}$	60	7.40	1.6	12.4	57.8	1.8	0.168	11.9	264	10730	573	22
(n = 48)	s	14	0.29	0.4	14.3	11.9	0.5	0.053	10.3	169	2869	315	25
Vertisols	$\bar{x}$	58	7.16	2.8	8.9	41.1	1.1	0.112	12.0	352	7256	681	104
(n = 135)	s	12	0.72	5.3	12.1	14.4	0.6	0.059	14.2	237	2854	451	278
Yermosols	$\bar{x}$	44	7.83	6.2	6.1	20.3	0.6	0.082	7.3	438	5268	480	447
(n = 92)	s	10	0.24	9.7	4.3	10.6	0.2	0.020	7.8	307	1770	270	591
Xerosols	$\bar{x}$	48	7.62	4.4	12.4	29.0	0.8	0.096	13.5	601	6207	659	227
(n = 101)	s	13	0.27	5.9	13.7	10.5	0.3	0.032	15.1	344	2300	362	301

Table 9. Properties and nutrients of soils classified in 1974 by FAO/UNESCO [Sillanpää, 1982 #18]

Total Flux (GtC/y) in each Holdridge life-zone: PCO2 REGRESSION FOR UNKNOWN LIF-ZONES									
HLZ	Flux(Rg,Kh,K1,K2)			Flux(Rtot,Kh,K1,K2)			Flux(Rg,Kh only)		
#	Primary	Upper	Lower	Primary	Upper	Lower	Primary	Upper	Lower
*1	0	0	0	0	0	0	0	0	0
*2	0	0	0	0	0	0	0	0	0
*3	0.00427	0.018749	0.002194	0.042697	0.187486	0.021939	0.003157	0.004447	0.002113
4	0.005268	0.053461	0.001029	0.015495	0.157237	0.003027	0.002804	0.005933	0.00094
*5	0.000066	0.00029	0.000034	0.00066	0.0029	0.000339	0.000049	0.000069	0.000033
*6	0.000002	0.000009	0.000001	0.000002	0.000009	0.000001	0.000002	0.000002	0.000001
*7	0.000104	0.000472	0.000053	0.001042	0.004717	0.00053	0.000076	0.000106	0.000051
*8	0.199665	2.087905	0.039732	1.197989	12.527428	0.238389	0.042107	0.059074	0.028289
9	0.638399	10.939685	0.04955	1.536844	26.414194	0.118186	0.088341	0.18626	0.029751
*10	0.003195	0.008946	0.001032	0.039245	0.357688	0.008392	0.003059	0.006441	0.00103
*11	0.000704	0.008028	0.000107	0.000704	0.008028	0.000107	0.000093	0.000129	0.000063
*12	0.001873	0.021365	0.000284	0.001873	0.021365	0.000284	0.000246	0.000343	0.000167
13	0.008414	0.155381	0.000471	0.180165	3.290722	0.010697	0.000552	0.001152	0.000187
14	0.737053	3.038445	0.223124	2.647136	10.063649	0.815979	0.650424	1.359458	0.219956
15	0.011961	0.077977	0.003129	0.059807	0.389886	0.015647	0.008907	0.01853	0.003014
*16	0.008997	0.015186	0.005948	0.053981	0.091117	0.035691	0.008766	0.012206	0.005932
*17	0.005064	0.059	0.000721	0.005064	0.059	0.000721	0.000582	0.000802	0.000398
*18	0.004418	0.051471	0.000629	0.004418	0.051471	0.000629	0.000508	0.000699	0.000348
19	0.007543	0.141007	0.00041	0.007543	0.141007	0.00041	0.00045	0.000927	0.000154
20	0.003281	0.026721	0.000763	0.017485	0.137169	0.004163	0.002139	0.004467	0.000723
21	0.081505	0.438945	0.023042	0.259185	1.395846	0.073274	0.066016	0.136476	0.022471
*22	0.027733	0.081022	0.016716	0.055465	0.162043	0.033432	0.024042	0.033087	0.01645
*23	0.011001	0.03214	0.006631	0.022002	0.064279	0.013262	0.009537	0.013125	0.006525
*24	0.000327	0.003834	0.000046	0.000327	0.003834	0.000046	0.000036	0.00005	0.000025
*25	0.001678	0.019667	0.000235	0.003356	0.039334	0.00047	0.000186	0.000255	0.000128
26	0.000398	0.005516	0.000054	0.002783	0.038612	0.000378	0.000129	0.000265	0.000044
27	0.174876	0.369153	0.060425	0.87438	1.845764	0.302126	0.174068	0.353659	0.060425
*28	0.312371	0.603698	0.205221	1.093298	2.112943	0.718272	0.297298	0.407644	0.204136
29	0.094935	0.306412	0.031012	0.449994	1.452391	0.146996	0.088475	0.179571	0.030784
*30	0.027088	0.05235	0.017796	0.054175	0.1047	0.035592	0.02578	0.035349	0.017702
31	0.000934	0.017381	0.000054	0.004672	0.086907	0.000268	0.000066	0.000134	0.000023
*32	0.000838	0.009969	0.000112	0.001675	0.019939	0.000224	0.000083	0.000113	0.000058
*33	0.002786	0.03316	0.000372	0.006964	0.0829	0.00093	0.000277	0.000375	0.000192
34	0.275563	1.252479	0.082703	0.386077	1.754787	0.115871	0.236229	0.484281	0.081339
35	0.8998	5.466449	0.247774	5.071657	31.000368	1.393297	0.692782	1.409249	0.240365
36	0.424436	1.24626	0.140328	1.788188	5.162614	0.592648	0.402504	0.819132	0.1393
*37	0.405162	0.805853	0.267698	0.810324	1.611706	0.535396	0.38323	0.519289	0.266127
*38	0.018225	0.036248	0.012041	0.036449	0.072496	0.024083	0.017238	0.023358	0.011971
Totals									
	4.4	**27.485**	**1.441**	**16.733**	**100.917**	**5.262**	**3.23**	**6.076**	**1.391**

Table 11. Total carbon flux in each Holdridge life-zone calculate from PCO_2 regression

Table 12. Flux from regressions with PCO_2, and from the average DIC for unknown life-zones

Total Flux (GtC/y) in each Holdridge life-zone: DIC AVERAGES FOR UNKNOWN LIFE-ZONES										
HLZ	Flux(Rg,Kh,K1,K2)			Flux(Rtot,Kh,K1,K2)			Flux(Rg,Kh only)			
#	Primary	Upper	Lower	Primary	Upper	Lower	Primary	Upper	Lower	
*1	0	0	0	0	0	0	0	0	0	
*2	0	0	0	0	0	0	0	0	0	
*3	0.027126	0.345874	0.004192	0.271263	3.458744	0.041925	0.010579	0.021847	0.003615	
4	0.013144	0.205717	0.001315	0.038659	0.605051	0.003869	0.002804	0.005933	0.00094	
*5	0.000299	0.003815	0.000046	0.002992	0.038148	0.000462	0.000117	0.000241	0.00004	
*6	0.000013	0.000172	0.000002	0.000013	0.000172	0.000002	0.000005	0.000011	0.000002	
*7	0.000643	0.008202	0.000099	0.006433	0.082018	0.000994	0.000251	0.000518	0.000086	
*8	0.319133	4.069111	0.049323	1.914795	24.414664	0.295938	0.124459	0.257023	0.042531	
9	0.143362	1.248149	0.031749	0.136364	0.291541	0.045714	0.088341	0.18626	0.029751	
*10	0.003296	0.010952	0.001038	0.039749	0.367715	0.008423	0.003059	0.006441	0.00103	
*11	0.000803	0.010236	0.000124	0.000803	0.010236	0.000124	0.000313	0.000647	0.000107	
*12	0.00202	0.02575	0.000312	0.00202	0.02575	0.000312	0.000788	0.001626	0.000269	
13	0.008414	0.155381	0.000471	0.180165	3.290722	0.010697	0.000552	0.001152	0.000187	
14	1.124905	10.5888	0.237156	3.676427	30.110003	0.853249	0.650424	1.359458	0.219956	
15	0.029201	0.41304	0.003752	0.146003	2.065202	0.018761	0.008907	0.01853	0.003014	
*16	0.013264	0.169122	0.00205	0.079584	1.014734	0.0123	0.005173	0.010683	0.001768	
*17	0.004662	0.059447	0.000721	0.004662	0.059447	0.000721	0.001818	0.003755	0.000621	
*18	0.003845	0.04902	0.000594	0.003845	0.04902	0.000594	0.001499	0.003096	0.000512	
19	0.007543	0.141007	0.000409	0.007543	0.141007	0.000409	0.00045	0.000927	0.000154	
20	0.008113	0.089187	0.001493	0.02999	0.411023	0.004066	0.003946	0.008203	0.001341	
21	0.081505	0.438945	0.023042	0.259185	1.395846	0.073274	0.066016	0.136476	0.022471	
*22	0.033559	0.427892	0.005187	0.067118	0.855785	0.010373	0.013088	0.027028	0.004472	
*23	0.002194	0.027975	0.000339	0.004388	0.05595	0.000678	0.000856	0.001767	0.000292	
*24	0.00028	0.003573	0.000043	0.00028	0.003573	0.000043	0.000109	0.000226	0.000037	
*25	0.001359	0.017326	0.00021	0.002718	0.034651	0.00042	0.00053	0.001094	0.000181	
26	0.000398	0.005516	0.000054	0.002783	0.038612	0.000378	0.000129	0.000265	0.000044	
27	0.174876	0.369153	0.060425	0.87438	1.845764	0.302126	0.174068	0.353659	0.060425	
*28	0.988314	12.601527	0.152747	3.459098	44.105346	0.534615	0.385433	0.795969	0.131712	
29	0.094935	0.306412	0.031012	0.449994	1.452391	0.146996	0.088475	0.179571	0.030784	
*30	0.005734	0.073117	0.000886	0.011469	0.146234	0.001773	0.002236	0.004618	0.000764	
31	0.001136	0.021386	0.000061	0.005681	0.10693	0.000305	0.000066	0.000134	0.000023	
*32	0.000529	0.006739	0.000082	0.001057	0.013479	0.000163	0.000206	0.000426	0.00007	
*33	0.001571	0.020028	0.000243	0.003927	0.050069	0.000607	0.000613	0.001265	0.000209	
34	0.548624	6.594914	0.092593	0.76865	9.239809	0.129728	0.236229	0.484281	0.081339	
35	0.880402	5.084852	0.247088	4.969923	28.998987	1.389702	0.692782	1.409249	0.240365	
36	0.706097	2.147504	0.232244	1.506527	4.261371	0.500732	0.665531	1.353965	0.230141	
*37	0.074049	0.944161	0.011444	0.148097	1.888322	0.022889	0.028878	0.059637	0.009868	
*38	0.000748	0.009537	0.000116	0.001496	0.019074	0.000231	0.000292	0.000602	0.0001	
Totals										
	5.31	**46.69**	**1.19**	**19.08**	**160.95**	**4.41**	**3.26**	**6.7**	**1.12**	

Result Summary

			Results from calculation with PCO2			Results from calculation with average DIC		
Holdridge life-zone		Area	Total Flux	Flux/Area	log(Flux/Area)	Total Flux	Flux/Area	log(Flux/Area)
#	Name	(10^12 m^2)	(GtC/y)	(kg/m^2/y)		(GtC/y)	(kg/m^2/y)	
*1	Ice	2.042	0	0		0	0	0
*2	Dry tundra	0	0	0		0	0	0
*3	Moist tundra	2.722	0.00427	0.00157	-2.804	0.027126	0.00997	-2.001
4	Wet tundra	1.505	0.005268	0.0035	-2.456	0.013144	0.00873	-2.059
*5	Rain tundra	0.03	0.000066	0.0022	-2.658	0.000299	0.00997	-2.001
*6	Boreal desert	0.027	0.000002	0.00007	-4.155	0.000013	0.00048	-3.319
*7	Boreal dry bush	1.292	0.000104	0.00008	-4.097	0.000643	0.0005	-3.301
*8	Boreal moist forest	12.801	0.199665	0.0156	-1.807	0.319133	0.02493	-1.603
9	Boreal wet forest	4.289	0.638399	0.14885	-0.827	0.143362	0.03343	-1.476
*10	Boreal rain forest	0.308	0.003195	0.01037	-1.984	0.003296	0.0107	-1.971
*11	Bool temperate desert	1.613	0.000704	0.00044	-3.357	0.000803	0.0005	-3.301
*12	Cool temperate desert bush	4.046	0.001873	0.00046	-3.337	0.00202	0.0005	-3.301
13	Cool temperate steppe	9.18	0.008414	0.00092	-3.036	0.008414	0.00092	-3.036
14	Cool temperate moist forest	9.358	0.737053	0.07876	-1.104	1.124905	0.12021	-0.92
15	Cool temperate wet forest	1.642	0.011961	0.00728	-2.138	0.029201	0.01778	-1.75
*16	Cool temperate rain forest	0.266	0.008997	0.03382	-1.471	0.013264	0.04986	-1.302
*17	Warm temperate desert	9.35	0.005064	0.00054	-3.268	0.004662	0.0005	-3.301
*18	Warm temperate desert bush	7.705	0.004418	0.00057	-3.244	0.003845	0.0005	-3.301
19	Warm temperate thorn steppe	7.702	0.007543	0.00098	-3.009	0.007543	0.00098	-3.009
20	Warm temperate dry forest	9.691	0.003281	0.00034	-3.469	0.008113	0.00084	-3.076
21	Warm temperate moist forest	9.307	0.081505	0.00876	-2.057	0.081505	0.00876	-2.057
*22	Warm temperate wet forest	0.673	0.027733	0.04121	-1.385	0.033559	0.04986	-1.302
*23	Warm temperate rain forest	0.044	0.011001	0.25002	-0.602	0.002194	0.04986	-1.302
*24	Subtropical desert	0.562	0.000327	0.00058	-3.237	0.00028	0.0005	-3.301
*25	Subtropical desert bush	0.545	0.001678	0.00308	-2.511	0.001359	0.00249	-2.604
26	Subtropical thorn woodland	1.415	0.000398	0.00028	-3.553	0.000398	0.00028	-3.553
27	Subtropical dry forest	4.936	0.174876	0.03543	-1.451	0.174876	0.03543	-1.451
*28	Subtropical moist forest	9.905	0.312371	0.03154	-1.501	0.988314	0.09978	-1.001
29	Subtropical wet forest	0.929	0.094935	0.10219	-0.991	0.094935	0.10219	-0.991
*30	Subtropical rain forest	0.023	0.027088	1.17774	0.071	0.005734	0.2493	-0.603
31	Tropical desert	1.447	0.000934	0.00065	-3.187	0.001136	0.00079	-3.102
*32	Tropical desert bush	0.212	0.000838	0.00395	-2.403	0.000529	0.0025	-2.602
*33	Tropical thorn woodland	0.315	0.002786	0.00884	-2.054	0.001571	0.00499	-2.302
34	Tropical very dry forest	1.461	0.275563	0.18861	-0.724	0.548624	0.37551	-0.425
35	Tropical dry forest	6.514	0.8998	0.13813	-0.86	0.880402	0.13516	-0.869
36	Tropical moist forest	7.182	0.424436	0.0591	-1.228	0.706097	0.09831	-1.007
*37	Tropical wet forest	0.297	0.405162	1.36418	0.135	0.074049	0.24932	-0.603
*38	Tropical rain forest	0.003	0.018225	6.075	0.784	0.000748	0.24933	-0.603
	Totals	**131.339**	**4.4**	**0.0335**	**-1.475**	**5.31**	**0.0404**	**-1.394**

Table 13. Global flux and error bounds for different methods

Global Carbon Flux Parameters used in calculation	Method for determining Flux for Life-zones without PCO2 data	Best estimate (GtC/y)	Error estimate	
			Upper Bound	Lower Bound
Rg, Kh, K1, K2	(*)PCO2 regression	(*)4.4	27.5	1.4
	DIC averaging	5.31	46.69	1.19
Rtotal, Kh,K1, K2	PCO2 regression	13.7	100.9	5.3
	DIC averaging	19.1	161	4.4
Rg, Kh only	PCO2 regression	3.2	6.1	1.4
	DIC averaging	3.3	6.7	1.1

Ised in making the map of carbon flux per area

Table 14. Total global flux result: summary

Bibliography

Boynton, D. and O.C. Compton. "Normal seasonal changes in oxygen and CO_2 percentages in gas from the larger pores of three orchard soils." *Soil Science* 57 (1944): 107-117.

Brady, N.C. and R.R. Weil. *The Nature and Properties of Soils*. Upper Saddle River, New Jersey: Prentice Hall, 1996.

Bridges, E.M. *World Soils*. 3 ed. Cambridge, U.K.: Cambridge University Press, 1997.

Brook, G.A., Folkoff, M.E., and E.O. Box. "A world model of soil carbon dioxide." *Earth Surface Processes and Landforms* 8 (1983): 79-88.

Butler, J.N. *Carbon Dioxide Equilibria and their Applications*. Reading, Massachusetts: Addison-Wesley, 1982.

Buyanovsky, G.A. and G.H. Wagner. "Annual cycles of carbon dioxide levels in soil air." *Soil Science Society of America Journal* 47 (1983): 1139-1145.

Cerling, T.E., Solomon, D.K., Quade, J., and J.R. Bowman. "On the isotopic composition of carbon in soil carbon dioxide." *Geochimica et Cosmochimica Acta* 55 (1991): 3403-3405.

Davidson, E.A. and S.E. Trumbore. "Gas diffusivity and production of CO_2 in deep soils of the eastern Amazon." *Tellus* 47B (1995): 550-565.

Devol, A.H., Quay, P.D., and J.E. Richey. "The role of gas exchange in the inorganic carbon, oxygen and ^{222}Rn budgets of the Amazon River." *Limnology and Oceanography* 32, no. 1 (1987): 235-248.

Drever, J.I. *The Geochemistry of Natural Waters: Surface and Groundwater Environments.* Upper Saddle River, New Jersey: Prentice Hall, 1997.

FAO/UNESCO. "Soil Map of the World." : FAO/UNESCO, 1974.

Hendry, M.J., Lawrence, G.J., and S. Ephraums. "Greenhouse Gases and Aerosols." In *Climate Change 1990: IPCC Scientific Assessment*, 7-39. Cambridge, U.K.: University Press, 1990.

Hendry, M.J., Lawrence, J.R., Zanyk, B.N., and R. Kirkland. "Microbial production of CO_2 in unsaturated geologic media in a mesoscale model." *Water Resources Research* 29, no. 4 (1993): 973-984.

Hinkle, M.E. "Environmental conditions affecting concentrations of He, CO_2, O_2 and N_2 in soil gases." *Applied Geochemistry* 9 (1994): 55-63.

Holdridge, L.R. "Determination of world plant formations from simple climatic data." *Science* 105 (1947): 367-368.

Holdridge, L.R. "The world life-zone classification system and forestry research." In *Proceedings of the 7th World Forestry Congress*. Buenos Aires, 1972.

Holmgren, G.G.S., Meyer, M.W., Chaney, R.L., and R.B. Daniels. "Cadmium, lead, zinc, copper and nickel in agricultural soils in the United States of America." *Journal of Environmental Quality* 22 (1993): 335-348.

Houghton, J.T., Filho, L.G.M., Bruce, J., Hoesung Lee, Callander, B.A., Haites, E., Harris, N. and Maskell, K., ed. *Climate Change 1994: Radiative Forcing of Climate Change and An evaluation of the IPCC IS92 Emission Scenarios*. Cambridge, U.K.: University of Cambridge Press, 1995.

Jugsujinda, A., Delaune, R.D., Lindau, C.W., Sulaeman, E., and S.R. Pezeshki. "Factors controlling carbon dioxide and methane production in acid sulfate soils." *Water, Air, and Soil Pollution* 87 (1996): 345-355.

Keller, C.K. "Hydrogeochemistry of a clayey till 2: Sources of CO_2." *Water Resources Research* 27, no. 10 (1991): 2555-2564.

Korzoun, V.I., Sokolov, A.A., Budyko, M.I., Voskresensky, K.P., Kalinin, G.P., Konoplyantsev, A.A., Korotkevich, E.S., and M.I. L'vovich, ed. *Atlas of World Water Balance*. Paris: UNESCO Press, 1977.

Kunkler, J.L. "The sources of carbon dioxide in the zone of aeration of the bandelier tuff, near Los Alamos, New Mexico." In *U.S. Geological Survey Professional Paper 650-B*, B185-B188, 1969.

L'vovich, M.I. *World Water Resources and Their Future*. Translated by R.L. Nace. Chelsea, Michigan: American Geophysical Union, 1979.

Leeman, R. , 1999.

Lovell, J.S., Hale, M., and J.S. Webb. "Soil air carbon dioxide and oxygen measurements as a guide to concealed mineralization in semi-arid regions." *Journal of Geochemical Exploration* 19 (1983): 305-317.

Nepstad, D.C., de Carvalho, C.R., Davidson, E.A., Jipp, P.H., Lefebvre, P.A., Negreiros, G.H., da Silva, E.D., Stone, T.A., Trumbore, S.E., and S. Vieira. "The role of deep roots in the hydrological and carbon cycles of Amazonian forests and pastures." *Nature* 372, no. 15 December (1994): 666-669.

Plummer, L.N. and E. Busenberg. "The solubility's of calcite, aragonite, and vaterite in CO_2-H_2O between 0 and 90 ^{0}C and an evaluation of the aqueous model for the system $CaCO_3$-CO_2-H_2O." *Geochimica et Cosmochimica Acta* 44 (1982): 1723-1735.

Post, W.M., Emanuel, W.R., Zinke, P.J. and A. G. Stangenberger. "Soil carbon pools and world life-zones." *Nature (London)* 298, no. 5870 (1982): 156-159.

Prentice, I.C., Cramer, W., Harrison, S.P., Leemans, R., Monserud, R.A., and A.M. Solomon. "A global biome model based on plant physiology and dominance, soil properties and climate." *Journal of Biogeography* 19 (1992): 117-134.

Reardon, E.J., Allison, G.B. and P. Fritz. "Seasonal chemical and isotopic variations of soil CO_2 at trout creek, Ontario." *Journal of Hydrology* 43 (1979): 355-371.

Russel, E.W. *Soil condition and plant growth.* London: Longmans, 1973.

Shiklomanov, I.A. and A.A. Sokolov. "New Approaches in Water Balance Computations: Methodological basis of world water balance investigation and computation." A paper delivered at the Hamburg Workshop, August 1983, 1983.

Sillanpää, M. *Micronutrients and the nutrient status of soils: a global study.* Rome: FAO, 1982.

Solomon, D.K. and T.E. Cerling. "The annual carbon dioxide cycle in a montane soil: observations, modeling, and implications for weathering." *Water Resources Research* 23, no. 12 (1987): 2257-2265.

Suchet, P.A. and J.L. Probst. *A Global 1 degree by 1 degree distribution of atmospheric/soil CO_2 consumption by continental weathering and of riverine HCO_3 yield.* Stasbourg Cedex, France: Centre National de la Recherche Scientifique, Center de Geochemie de la Surface, Carbon Dioxide Information Analysis Center, 1995.

Thorstenson, D.C., Weeks, E.P., Haas, H., and D.W. Fisher. "Distribution of gaseous $^{12}CO_2$, $^{13}CO_2$, and $^{14}CO_2$ in the sub-soil unsaturated zone of the western U. S. Great Plains." *Radiocarbon* 25, no. 2 (1983): 315-346.

van Breemen, N., and T.C.J. Feijtel. "Soil processes and properties involved in the production of greenhouse gases, with special relevance to soil taxonomic systems." In *Soils and the Greenhouse Effect*, ed. A.F. Bouwman. (1989: Wegeningen, Netherlands): John Wiley and Sons, Ltd., 1990.

Vorobyoua, L.A., Krechetova, Y.V., and Y.Y. Goronenkau. "Carbonate equilibria and alkalinity of soils of Djanybek Experimental Station." *Moscow University Soil Science Bulletin* 46, no. 4 (1991): 17-22.

Wallick, E.I. "Chemical evolution of groundwater in a drainage basin of Holocene age, East-central Alberta, Canada." *Journal of Hydrology* 54 (1981): 245-283.

Wood, B.D., Keller, C.K., and D.L. Johnstone. "In situ measurement of microbial activity and controls on microbial CO_2 production in the unsaturated zone." *Water Resources Research* 29, no. 3 (1993): 647-659.